This Page Is Inserted by IFW Operations
and is not a part of the Official Record

BEST AVAILABLE IMAGES

Defective images within this document are accurate representations of the original documents submitted by the applicant.

Defects in the images may include (but are not limited to):

- BLACK BORDERS
- TEXT CUT OFF AT TOP, BOTTOM OR SIDES
- FADED TEXT
- ILLEGIBLE TEXT
- SKEWED/SLANTED IMAGES
- COLORED PHOTOS
- BLACK OR VERY BLACK AND WHITE DARK PHOTOS
- GRAY SCALE DOCUMENTS

IMAGES ARE BEST AVAILABLE COPY.

As rescanning documents *will not* correct images, please do not report the images to the Image Problem Mailbox.

Functional correction of established central nervous system deficits in an animal model of lysosomal storage disease with feline immunodeficiency virus-based vectors

Andrew I. Brooks*†‡, Colleen S. Stein§, Stephanie M. Hughes§, Jason Heth¶, Paul M. McCray, Jr.‖, Sybille L. Sauter**, Julie C. Johnston**, Deborah A. Cory-Slechta*†, Howard J. Federoff†‡††, and Beverly L. Davidson§††‡‡§§

Departments of §Internal Medicine, ‡‡Neurology, §§Physiology and Biophysics, ¶Neurosurgery, and ‖Pediatrics, University of Iowa Program in Gene Therapy, University of Iowa College of Medicine, Iowa City, IA 52242; *Department of Environmental Medicine, †Centers for Functional Genomics, and ‡Aging and Developmental Biology, University of Rochester Medical Center, Rochester, NY 14642; and **Chiron Technologies, Center for Gene Therapy, San Diego, CA 92121

Edited by Roscoe O. Brady, National Institutes of Health, Bethesda, MD, and approved February 20, 2002 (received for review January 8, 2002)

Gene transfer vectors based on lentiviruses can transduce terminally differentiated cells in the brain; however, their ability to reverse established behavioral deficits in animal models of neurodegeneration has not previously been tested. When recombinant feline immunodeficiency virus (FIV)-based vectors expressing β-glucuronidase were unilaterally injected into the striatum of adult β-glucuronidase deficient [mucopolysaccharidosis type VII (MPS VII)] mice, an animal model of lysosomal storage disease, there was bihemispheric correction of the characteristic cellular pathology. Moreover, after the injection of FIV-based vectors expressing β-glucuronidase into brains of β-glucuronidase-deficient mice with established impairments in spatial learning and memory, there was dramatic recovery of behavioral function. Cognitive improvement resulting from expression of β-glucuronidase was associated with alteration in expression of genes associated with neuronal plasticity. These data suggest that enzyme replacement to the MPS VII central nervous system goes beyond restoration of β-glucuronidase activity in the lysosome, and imparts improvements in plasticity and spatial learning.

Mucopolysaccharidosis type VII (MPS VII), or Sly syndrome, is a lysosomal storage disease (LSD) resulting from mutations in β-glucuronidase (1). Similar to many other LSDs, there are both systemic and central nervous system (CNS) components, and patients show progressive disease involvement. In β-glucuronidase deficiency, lysosomes become progressively laden with undegraded glycosaminoglycans, leading to mental retardation and loss of hearing and vision. Patients also suffer from dysostosis multiplex, joint abnormalities, and hepatosplenomegaly.

An animal model for MPS VII, the β-glucuronidase-deficient gus^{mps} mouse (2, 3), has been invaluable in testing enzyme, cell, and gene therapies (4–9). MPS VII mice exhibit progressive lysosomal accumulation in multiple organs, including but not limited to bone, spleen, liver, lung, kidney, retina, and brain (2, 10). Early work by Birkenmeier and colleagues (11, 12) demonstrated that enzyme replacement therapy or bone marrow transplant was sufficient for correction of the visceral manifestations of the disorder. However, there remained significant storage within the brain. Until recently, the functional affect of CNS storage was unknown. Recent work by Sands and coworkers (13) demonstrated that MPS VII mice have progressive learning impairment as measured by a Morris water maze, as well as gradual loss of vision. Protection against the onset of storage pathology and the functional deficits of learning impairment could be accomplished by enzyme therapy or adeno-associated viral (AAV)-mediated therapy, initiated immediately after birth (13–15). Similarly, in an animal model of metachromatic leukodystrophy, HIV-based vectors could protect against disease incipience (16).

The collective incidence of LSDs is ≈1 in 7,000 live births, with 65% affecting the CNS (17). In most instances, disease diagnosis occurs well after the onset of pathology. As such, recovery of function, rather than protection from disease onset, will be an important benchmark for efficacy of gene therapy for the LSDs. Our prior studies with recombinant adenoviruses, and others' using AAV- or HIV-based vectors, established that focal expression of β-glucuronidase within diseased rodent striata could reduce storage pathology in both hemispheres (4, 5, 8, 18). The enzyme is secreted from transduced cells and taken up by nontransduced cells, leading to a zone of correction that extends beyond the site of transduction. In this study we set out to test the hypothesis that recombinant viral vectors based on feline immunodeficiency virus (FIV) could revert not only the pathologic phenotype, but more importantly, the established behavioral dysfunction.

Materials and Methods

***In Vivo* Delivery and Transgene Assays.** Animal studies were approved by the Animal Care and Use Committee of the University of Iowa. β-Glucuronidase-deficient mice were from The Jackson Laboratories and our own breeding colony. C57BL/6 mice were from Harlan Sprague (Indianapolis, IN). For virus injections, mice were anesthetized with ketamine/xylazine (100–125 mg/kg ketamine/10–12.5 mg/kg xylazine). The bregma was exposed by incision and used as a zero coordinate for stereotactic injections into the striatum or ventricle as described (4, 19).

For histological studies, the mice were injected unilaterally with 5 μl [1×10^6 transducing units (TU)] of vector. Animals were killed 3, 6, 9, 15, and 18 weeks later, and their brains were analyzed for enzyme activity, volume, *in situ* RNA hybridization, and storage vacuoles as described (4).

Vectors. FIV packaging constructs were generated from the full-length FIV molecular clone, FIV-34TF10 (National Institutes of Health AIDS Research and Reference Reagent Program), as described (20). The FIV construct, $pVET_LC\beta gal$ ($pVET_LC\beta$; ref. 20), was generated by inserting cytomegalovirus (CMV)-β-galactosidase into the $pVET_L$ FIV backbone. To construct

This paper was submitted directly (Track II) to the PNAS office.

Abbreviations: MPS VII, Mucopolysaccharidoses type VII; FIV, feline immunodeficiency virus; LSD, lysosomal storage disease; CNS, central nervous system; TU, transducing units; CMV, cytomegalovirus; RAPC, repeated acquisition and performance chamber; RA, repeated acquisition; P, performance; QPCR, quantitative real time PCR; MCS, multiple cloning site; RSV, Rous sarcoma virus.

See commentary on page 5760.

††To whom reprint requests may be addressed. E-mail: beverly-davidson@uiowa.edu or howard_federoff@urmc.rochester.edu.

The publication costs of this article were defrayed in part by page charge payment. This article must therefore be hereby marked "*advertisement*" in accordance with 18 U.S.C. §1734 solely to indicate this fact.

www.pnas.org/cgi/doi/10.1073/pnas.082011999

pVET$_L$RβgIuc, a Rous sarcoma virus (RSV) promoter was isolated from pUC19RSV (J. K. Yee, personal communication), and the resulting fragment was inserted into pVET$_L$ to generate pVET$_L$RSV. The β-glucuronidase cDNA was isolated from pAdRSV4 (21) and ligated into pVET$_L$RSV to make pVET$_L$RβgIuc(+polyA). The poly(A) tail was removed to generate pVET$_L$RβgIuc. For FIVMCS, PVET$_L$RSV was modified to contain a multiple cloning site (MCS) downstream from the RSV promoter. The vesicular stomatitis virus (VSV)-G envelope plasmid, pCMV-G, has been described (22). Pseudotyped FIV vectors expressing β-glucuronidase (FIVβgluc) and β-galactosidase (FIVβgal) vector particles were done by transient transfection of plasmids into 293T cells plated one day earlier at 2.8×10^6 cells per 10-cm dish. Cotransfections were made with a 1:2:1 molar ratio of FIV packaging, FIV vector, and pCMV-G constructs. Harvested supernatants (32 and 48 h later) were passed through 0.45-μm Nalgene filters and concentrated by centrifugation (23). Vector titers determined by serial dilution on HT1080 cells and by quantitative PCR of transduced target cells ranged from 1×10^8 to 2×10^8 TU/ml (20).

Repeated Acquisition and Performance Chamber (RAPC) Analyses. The RAPC used to assess spatial learning and memory was done essentially as described (24–26). Mice ($n = 8$ each; MPS VII and control mice) were habituated to a reward solution before introduction to the RAPC. The habituation protocol required water deprivation for 12–16 h followed by exposure to a 0.2% saccharin solution for 30 min twice a day for 2 days, after which regular drinking water was provided *ad libitum*. Mice were introduced to the RAPC during four habituation sessions followed by four baseline experimental sessions (see Fig. 3, baseline sessions 1–4). A 12-h water deprivation period preceded behavioral sessions, with *ad libitum* water on nontest days. A session was 3 presentations each of the repeated acquisition (RA) component and the performance (P) component with 3 trials per presentation. In the RA component, the specific door sequence changed unpredictably with each successive session. During all P component sessions, the sequence of doors leading to the saccharin reward was identical. A discriminative stimulus (static audio signal) was played to signal that the P component was in effect. Thus, there were a total of 18 trials per session (3 trials per presentation × 3 presentations per component × 2 components per session). Latency was measured as the time required for the mouse to leave the start box, navigate through the four compartments, and consume the saccharin solution in the goal box. Mice were placed manually in the goal box if they failed to reach it within 10 min on any trial. Errors were defined as attempts to go through a locked door. Five weeks after the pretreatment sessions, MPS VII and control mice were split into groups ($n = 4$ per each treatment) and injected with FIVβgluc or FIVβgal (1×10^6 TU) into the striatum. Four weeks later, mice were reassessed according to the above protocol. Sessions 4, 5, and 6 were separated by 3 days each. A timeline for behavioral testing is detailed in Fig. 3*A*.

Statistics for Behavioral Analyses. Baseline differences (pretreatment) in errors and latencies were evaluated by using repeated-measures ANOVA (RMANOVA) with component (RA and P) and session (1–4) as within group factors and β-glucuronidase status (control vs. MPS VII) as a between-group factor. These were followed, where appropriate, by one-factor ANOVAs (β-glucuronidase status) for individual session data. Statistical assessment of changes in these measures after treatment were carried out separately for each treatment (FIVβgal and FIVβgluc) and for each component (RA and P) in RMANOVAs with β-glucuronidase status (control vs. MPS VII) as a between-group factor and session as within group factors. Subsequent one-factor ANOVAs were used, where appropriate, for determining differences between control vs. MPS VII groups for each session.

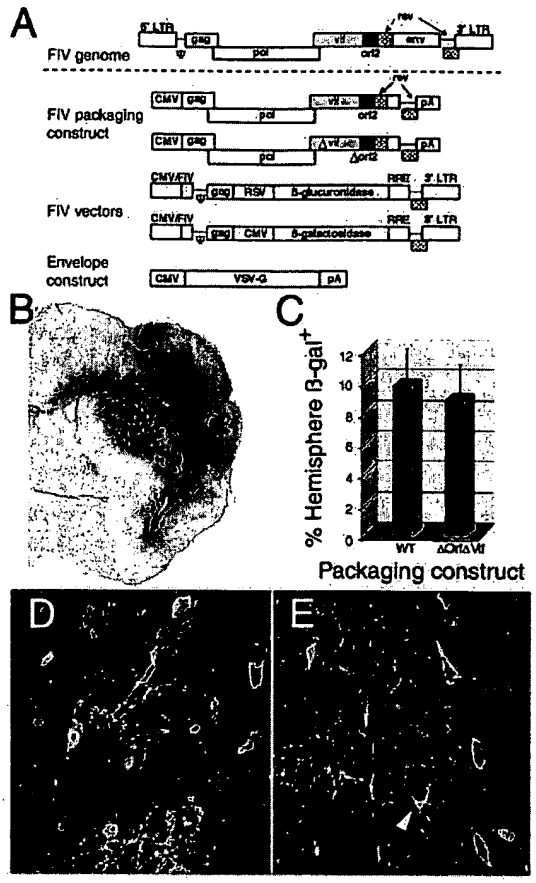

Fig. 1. FIV accessory proteins are not required for transduction of rodent CNS. FIV vectors encoding β-galactosidase containing both or neither of the Vif and Orf2 accessory proteins were generated as described (*Materials and Methods*) and injected into mice striata. (*A*) FIV packaging, vector, and envelope constructs. (*B*) Photomicrograph of a representative section stained for β-galactosidase activity. Mice were injected with FIVβgalΔvifΔorf2 18 weeks earlier. (*C*) The volume of β-galactosidase expression in FIV-injected hemispheres. (*D*) A representative confocal photomicrograph of the injected striatum after immunohistochemical staining for β-galactosidase (green) and NeuN (red) antigens. Cell soma colabeled for β-galactosidase and NeuN appear yellow in this merged image. (*E*) Occasional transduced glia could be identified in sections stained for glial fibrillary acid protein (GFAP, red) and β-galactosidase (green; arrowhead).

Microarray Study. Both striata of 16-week-old mice were injected with either 5 μl of FIVβgluc or FIVMCS (5×10^5 to 1×10^6 TU total; $n = 8$ per treatment). Eight weeks later the mice were killed, the brain was removed, meninges were dissected away, and brains were cut at the level of the dorsal hippocampus midsagitally. Hippocampi were removed, and before total RNA isolation, two groups of four hippocampi each were pooled, homogenized in Trizol (GIBCO/BRL) by using a Pro-200 homogenizer (PRO Scientific, Oxford, CT) and frozen on liquid nitrogen. RNA was prepped by using the standard Trizol protocol and assessed by gel electrophoresis and spectrophotometry. Target preparation was performed as directed (Affymetrix, Santa Clara, CA) with all components generated throughout the procedure (cDNA, full-length cRNA, and fragmented cRNA) analyzed by gel electrophoresis to assess size distribution.

Gene expression analysis was done by the Affymetrix Mu11K high-density oligonucleotide array at the University of Rochester Microarray Core Facility. Hybridization, staining, washing, and scanning were performed per the manufacturer's protocol. All

MEDICAL SCIENCES

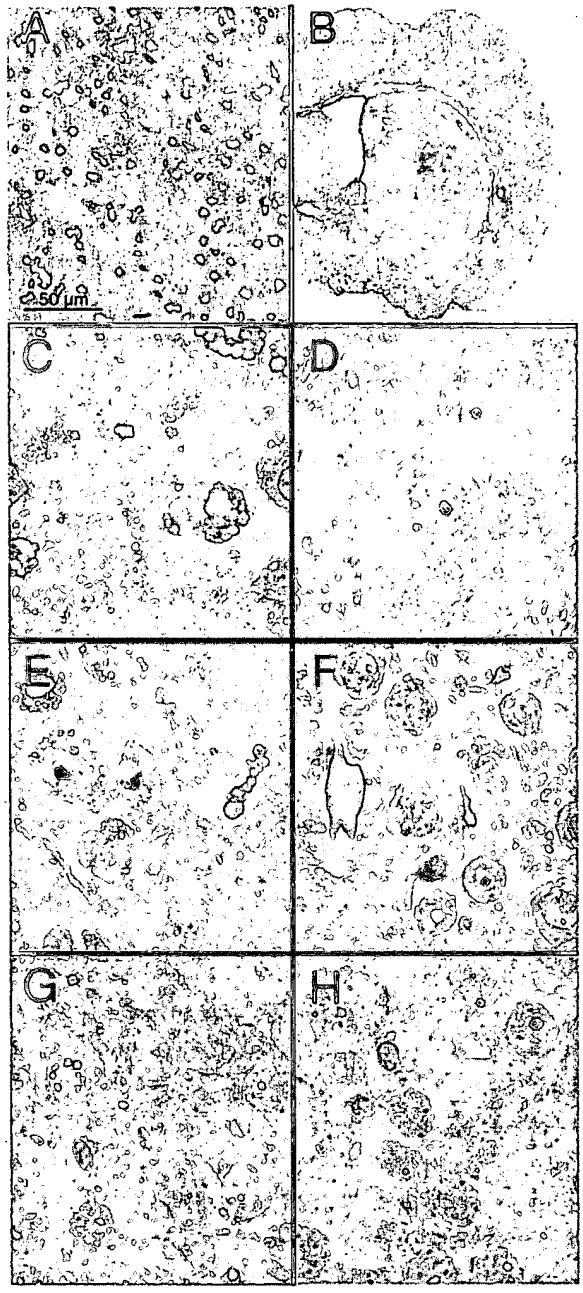

Fig. 2. β-Glucuronidase expression after FIV-mediated gene transfer. (*A*) Transgene-positive cells near the region of the injection as revealed by *in situ* RNA analyses. (*B*) β-Glucuronidase activity in the brain of a MPS VII mouse injected with FIVβgluc and stained for β-glucuronidase activity (dark red reaction product). (*C*, *E*, and *G*) Representative examples of the lysosomal storage in the striatum (*C*), cortex (*E*) and hippocampus (*G*) of 8- to 12-week-old MPS VII mice. (*D*, *F*, and *H*) Correction of the storage defect in the contralateral striatum (*D*), cortex (*F*) and hippocampus (*H*) 6 weeks after injection of FIVβgluc into an 8-week-old MPS VII mouse.

arrays were assessed for "array performance" by statistical analysis of control transcripts spiked into the hybridization mixture. In addition, several genes were identified on each array to assess the overall quality of array signal intensity. The results demonstrated that the arrays were within a 0.31-fold difference of each other at baseline, allowing for data normalization by the global scaling approach.

The Affymetrix Microarray Analysis Suite was used to generate the comparative analysis. The fold change represented for any transcript between the FIVMCS and FIVβgluc was calculated after global scaling to a target intensity of 2,500 (to normalize any differences in overall signal intensity among arrays). Super scoring was applied to all probe sets of 8 probe pairs or more. Data reported reflect the average fold changes in gene expression from two biological replicates (4 hippocampi each) for each condition. Data in Fig. 4*D* show the fold-change data from pair-wise comparisons of selected genes, of which all changed in the same direction. The false discovery rate of genes identified by our microarray analyses was determined by using significance analysis of microarrays (SAM) (27). A "two-class, unpaired" analysis within SAM was used to measure the effect of treatment as a function of genetically similar subjects (inbred strain, sex matched, littermates), and data were normalized by global scaling with $\Delta = 0.5$, based on the false positive distribution. By SAM, a total of 517 genes (4.7%) were called significant, and an additional 253 genes were called false positive. All genes discussed in Fig. 4 met SAM criteria for statistical significance.

Microarray Validation: Quantitative Real-Time PCR (QPCR) and Data Analysis. Levels of Pitpn (U96726), Fe65 (P46933), Fisp-12 (M70642), C/EBP (X61800), and Egr2 (Krox20, X06746) expression were examined in cDNAs archived from the microarray experiment by using TaqMan chemistry with specific probes and primers designed with PRIMER EXPRESS V.1.0. The following dye combinations were used: FAM (5-carboxyfluorescein; reporter), TAMRA (*N,N,N′,N′*-tetramethyl-6-carboxyrhodamine; quencher), and ROX (6-carboxy-X-rhodamine; reference). A validation experiment was done with a probe designed to glyceraldehyde-3-phosphate dehydrogenase (GAPDH) (M32599) to determine the relative probe efficiency. This probe was used as a reference gene for comparative analyses. The absolute value of the slope of log input amount vs. ΔC_T (C_T = threshold cycle) was less than 0.1 for all comparisons, allowing for $\Delta\Delta C_T$ determinations of relative quantitation of gene expression in FIVβgluc-treated mice vs. FIVMCS-treated mice (28). After optimization, cDNAs were diluted 1:100 with 1 μl used for each 25 μl PCR mixture containing 12.5 μl of ABI 2× Universal Master Mix, 1.25 μl of forward and reverse primers (final range 200–900, nM depending on primer set), and 1 μl of probe (final range 50–200 nM, depending on probe/primer set). Reactions were performed in triplicate and replicated three times. Thus, data in Table 1 reflect nine reactions per sample being tested; *t* test's for each sample achieved $P < 0.001$ or better. All reactions were run in an ABI 7700, and data were collected at all temperature phases during cycles. Raw data were analyzed by using the sequence detection software (Applied Biosystems) and relative quantitation using the comparative C_T method was performed in Microsoft EXCEL.

Results and Discussion

Evaluation of FIV Accessory Proteins for Gene Delivery to the CNS. FIV is distantly related to HIV. This nonprimate lentivirus does not replicate in human cells, and there has been no evidence of seroconversion among individuals exposed to FIV through repeated exposure by infected cats (29). FIV has two accessory proteins, Vif and Orf2. FIV Vif is the functional equivalent of HIV Vif, and is required for a productive infection in certain feline cells, for example, peripheral blood mononuclear cells (30, 31). FIV Orf2 is a weak transactivator of the FIV long terminal repeat (LTR), and therefore functionally similar to HIV Tat (32). We first determined whether Vif and Orf2 were required for gene transfer to mouse brain; vectors devoid of accessory proteins would be preferable if they are as functional as the parental vector *in vivo* (20). Because the FIV-based system uses a hybrid CMV/FIV LTR, we hypothesized that Orf2 would be dispensable, similar to that found *in vitro* (20). Recombinant FIV vectors expressing the reporter gene en-

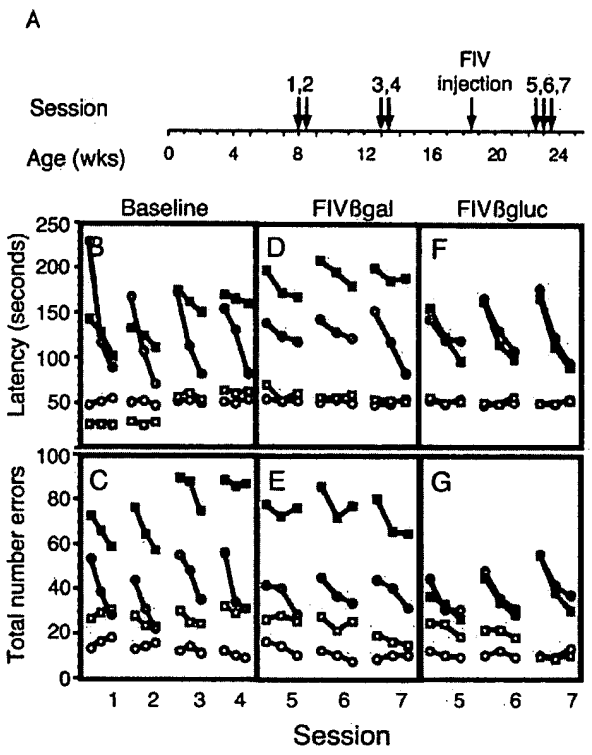

Fig. 3. Behavioral analyses in untreated and FIV-transduced mice. RAPC analysis was used to investigate baseline and posttreatment differences between MPS VII mice and age-matched heterozygous controls. (*A*) Behavioral sessions before and after gene transfer were performed according to the time line (*Materials and Methods*). MPS VII mice demonstrated significant baseline impairment in learning (solid red squares) relative to control mice (solid gray circles) as seen by both measures (latency in *B* and errors in *C*). There were no significant differences in the performance component of the assay between MPS VII (open red squares) and control (open gray circles) mice. After baseline testing, both groups were segregated randomly before bilateral striatal injection with FIVβgal or FIVβgluc. Behavioral tests on FIVβgal-treated (*D* and *E*) and FIVβgluc-treated (*F* and *G*) mice resumed 4 weeks after injection. FIVβgal-injected MPS VII mice continued to demonstrate a severe learning impairment in both latency and error (*D* and *E*). MPS VII mice injected with FIVβgluc exhibited no significant differences in learning compared with control mice in error or latency measures (*F* and *G*; $P \geq 0.05$), and reflect a recovery of the learning impairment seen in the baseline measurements (*B* and *C*). Solid symbols, learning component. Open symbols, performance component.

coding *Escherichia coli* β-galactosidase were generated by using the packaging constructs shown in Fig. 1*A* (20) and were injected into the striatum of mice. Full coronal sections were evaluated for β-galactosidase activity by histochemistry from 3 ($n = 6$; not shown) to 18 weeks ($n = 8$; Fig. 1*B*). In all cases, intrastriatal injections resulted in β-galactosidase activity in the ipsilateral striatum, corpus callosum, and the neocortex. Results with FIVβgalΔvifΔorf2 were not significantly different from FIVβgalwt ($P > 0.05$; Fig. 1*C*) as regards volume of transgene-positive brain (8.8 ± 2.4% and 9.7 ± 2.6% positive for FIVβgalΔvifΔorf2 and FIVβgalwt, respectively). Also, there was no decline in the β-galactosidase expression over time (8.8 ± 2.4% vs. 7.8 ± 1.7% positive at 3 and 18 weeks, respectively). Consistent with experiments with HIV-based vectors in rats (23), we found that the FIVβgal pseudotyped with the vesicular stomatitis virus (VSV)-G envelope readily transduced neuronal cells (Fig. 1*D*), with occasional glial fibrillary acidic protein, β-galactosidase double-positive (glial) cells also noted (Fig. 1*E*). Neuronal tropism was also found by using the amphotropic envelope from Moloney murine leukemia virus (data not shown).

FIV-Mediated Gene Transfer of β-Glucuronidase to MPS VII Mice. There are several important criteria for efficacy of FIV-mediated gene therapy to brain for treatment of the LSDs. First, does FIV-mediated gene transfer lead to adequate levels of β-glucuronidase expression for secretion and uptake into nearby nontransduced cells, and does the expressed enzyme lead ultimately to evidence of enzyme activity at sites distant from the injection? Second, is expression sufficient for reduction of the notable lysosomal pathology in affected brain in transduced and nontransduced cells? Finally, do FIV vectors expressing β-glucuronidase have a favorable impact on the disease course when introduced into animals with evident disease pathology and functional behavioral deficits? We first tested whether unilateral injection to the brains of 8-week-old MPS VII mice with the Vif- and Orf2-deleted FIVβgluc (Fig. 1*A*; $n = 6$) resulted in transduction of cells near the injection site. Although *in situ* hybridization for vector-encoded β-glucuronidase showed focal transduction (Fig. 2*A*), histological assay for β-glucuronidase (4) showed that levels of activity extended well beyond the area of transduced cells (Fig. 2*B*), with 18.1% ± 2.5% of the hemisphere positive for enzyme activity 18 weeks after vector introduction. In tissues from mice killed 3 weeks after gene transfer, histological correction of storage pathology was observed in the ipsilateral striatum and ipsilateral cortex, and modest reductions in storage product were seen in the contralateral cortex (data not shown). Six weeks after injection of FIVβgluc, there was notable correction of cellular morphology in regions of the injected (not shown) and contralateral hemispheres of the brain (Fig. 2 *D*, *F*, and *H*), as compared with the lysosome-laden cortical (Fig. 2*C*), striatal (Fig. 2*E*), or hippocampal (Fig. 2*G*) tissues from control MPS VII mice. The absence of lysosomal inclusions was maintained through the course of the study (18 weeks), supporting the hypothesis that persistent expression of β-glucuronidase from FIV-transduced cells, ≈2–5% of which may be secreted (13), resulted in correction of cells at increasing distances over time.

β-Glucuronidase-deficient mice have storage pathology in the eye and brain by several weeks after birth, leading to progressive decline in retinal and neuronal function as measured by electroretinograms or the Morris water maze, respectively (13, 33). By 8 weeks of age, there is sufficient motor impairment precluding further use of the Morris water maze. Thus, to test for functional recovery resulting from introduction of FIVβgluc into diseased mouse brain, the RAPC was used (24–26). The RAPC is a hippocampus-dependent paradigm that is capable of differentiating between spatial learning and other effects such as motor, motivational, and sensory disturbances that can confound analyses of spatial learning. Importantly, this testing paradigm allows for same-animal comparisons of pretreatment vs. posttreatment behavior in an environment devoid of strenuous physical activity.

Baseline testing. Behavioral testing using the RAPC was initiated on β-glucuronidase-deficient and age-matched heterozygous control littermates at 8 weeks of age, a time at which brain pathology is evident, to define baseline learning and performance abilities (Fig. 3*A*; *Materials and Methods*). Both latency (the time to reach the goal) and total errors (the number of mistakes made) were measured. In sessions 1 and 2, performed at 8 and 8.5 weeks of age, respectively, both MPS VII and control mice ($n = 8$ per group) showed reductions in the time to reach the goal box from the first to the last trial of each session (Fig. 3*B*). Similar results were seen for numbers of errors (Fig. 3*C*). However, the MPS VII mice showed significant impairments in learning relative to control mice (Fig. 3 *B* and *C*; $P = 0.0001$, $P = 0.029$ for latency and errors, respectively). At 13 and 13.5 weeks of age, β-glucuronidase-deficient mice showed further impairments in behavior, with increased latency and numbers of errors (sessions 3 and 4; Fig. 3 *B* and *C*). There was no evidence of impaired behavior of the control mice. Additionally, the relative difference in the performance component as compared with the learning component for either group remained unchanged ($P > 0.05$).

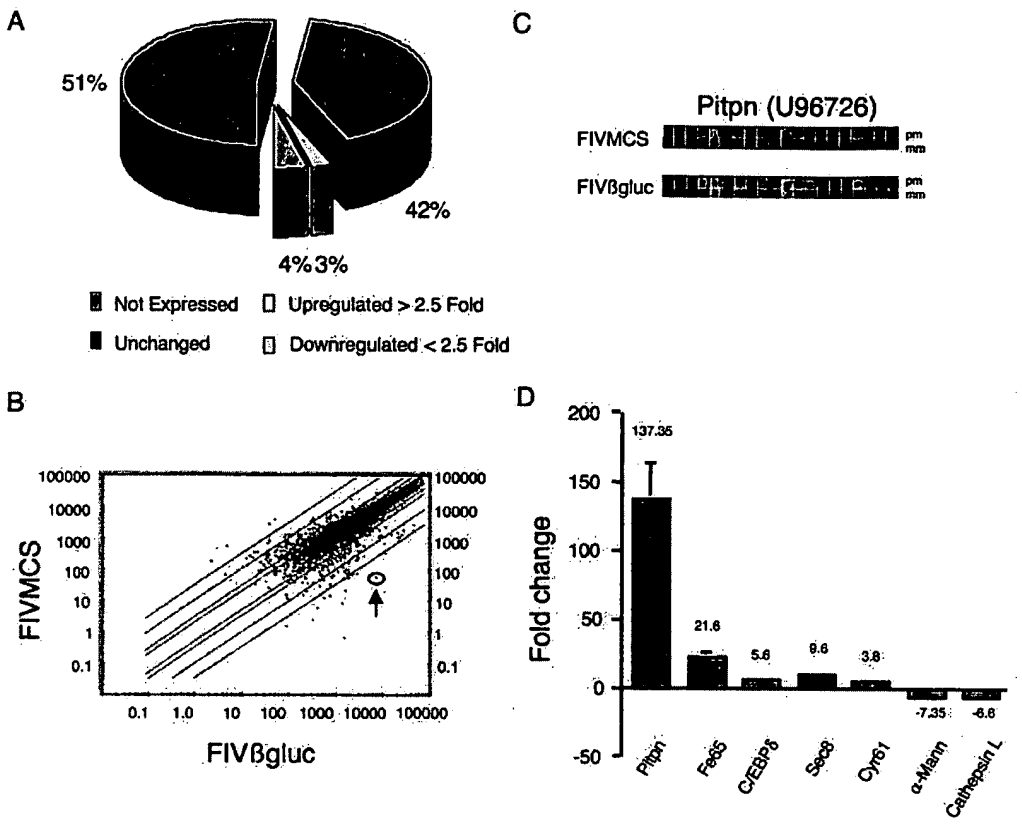

Fig. 4. Microarray analysis of murine hippocampus after treatment with FIV vectors. Hippocampi from FIVMCS- and FIVβgluc-treated animals were extracted 8 weeks after injection, and gene expression was analyzed on Affymetrix high-density oligonucleotide arrays. (*A*) A representation of the effects of FIVβgluc gene transfer on gene expression in the hippocampus. (*B*) A scatter plot depicts the average difference distribution of all genes examined, comparing FIVMCS with FIVβgluc samples. Red points depict genes that are called present, whereas blue points represent genes changing from absent to present or *vice versa*. Green lines indicate the magnitude of change with intervals of 2, 10, and 30-fold relative to baseline. One gene of interest, *Pitpn* (U96726), is circled in orange (arrow) and exhibits a significant change in gene expression as depicted by differences in the raw data images (*C*). (*C*) The increase in selective binding to the perfect match (pm) vs. the mismatch (mm) probes. (*D*) The increase or decrease in fold expression of RNA specific to selected genes from FIVβgluc relative to FIVMCS-treated mice. Data normalization and analyses were completed by using algorithms in the Affymetrix Microrarray Analysis suite and Data Mining Tools and significance analysis of microarrays (27).

Behavioral assays after FIV-mediated gene transfer. MPS VII and control mice were injected bilaterally at 18.5 weeks of age ($n = 4$ per group) with FIVβgluc or FIVβgal after baseline testing, with behavioral reassessment initiated 4 weeks later. β-Glucuronidase-deficient mice transduced with FIVβgluc showed dramatic improvements in latencies and errors to levels indistinguishable from controls (Fig. 3 *F* and *G*; $P > 0.05$). By contrast, FIVβgal-injected MPS VII mice continued to demonstrate severe learning impairments in error and latency measures relative to control mice (Fig. 3 *D* and *E*; $P = 0.0003$ and $P = 0.0019$ for error and latency, respectively). The data in Fig. 3 *F* and *G*, in concert with those shown in Fig. 2, suggest that therapies leading to reduction of storage pathology can significantly improve established learning deficits.

Molecular Correlates for Improved Pathology and Behavior. We next asked whether alterations in gene expression consistent with improvements in learning and memory or improvements in lysosomal function occurred as a result of FIVβgluc gene transfer. MPS VII mice (16 weeks of age) received intrastriatal injections of FIVβgluc or FIVMCS, a vector that expresses no transgene ($n = 8$ per group). FIVMCS, rather than FIVβgal, was used to avoid potential confounding effects caused by β-galactosidase expression. Eight weeks later, mice were killed, and RNA was isolated from dissected hippocampi. mRNAs were analyzed by using Affymetrix high-density oligonucleotide arrays.

After FIVβgluc injection into striatum, 93% of the genes and expressed sequence tags represented on the array did not change significantly relative to empty vector, or were not expressed, whereas 3% and 4% were up- or down-regulated greater than 2.5-fold, respectively (Fig. 4*A*). A scatter plot of average difference values between treatment groups illustrates the relative distribution of gene expression for the data set (Fig. 4*B*). Raw image data for *pitpn*, which encodes the α isoform of phosphatidylinositol transfer protein (PITPα), are shown in Fig. 4*C*. Reductions in *pitpn* expression occur in the mouse degeneration mutant *vibrator* (34), suggesting a requirement for PITPα in maintenance of neuronal function. In our studies, *pitpn* expression was increased approximately 137-fold relative to control tissues (Fig. 4*D*). QPCR validation studies confirmed elevated levels of mRNA specific to *pitpn* in isolated hippocampi (Table 1; refs. 28 and 35).

Although animals were killed 8 weeks after gene transfer, we found elevated expression of several genes implicated in learning and memory relative to FIVMCS-injected controls (Fig. 4*D*, Table 1). C/EBPδ has been shown to increase as a result of stimulation of cAMP signaling in hippocampal neurons (36, 37). In FIVβgluc-transduced mice, the expression of C/EPBδ was elevated 5.6- and 20-fold by microarray and QPCR analysis, respectively. *Egr2* (Krox 20), another immediate early gene implicated in learning and

Table 1. Validation of microarray data by QPCR

Gene of interest (GOI)	Treatment	GOI average C_T	GAPDH average C_T	ΔC_T GOI − GAPDH	$\Delta\Delta C_T$ $\Delta C_T - \Delta C_T$ MCS	Fold change relative to MCS
Pitpn (U96726)	FIVMCS	25.02 ± 0.80	19.18 ± 0.18	5.84 ± 0.82	0.00 ± 0.82	1.0
	FIVβgluc	20.07 ± 0.75	21.69 ± 0.46	−0.99 ± 0.89	−6.83 ± 0.88	114.04
Fe65 (P46933)	FIVMCS	28.62 ± 0.52	19.18 ± 0.18	9.44 ± 0.55	0.00 ± 0.55	1.0
	FIVβgluc	26.99 ± 0.77	21.69 ± 0.46	5.30 ± 0.90	−4.14 ± 0.90	17.67
C/EBPδ (X61800)	FIVMCS	31.71 ± 0.32	19.18 ± 0.18	12.53 ± 0.37	0.00 ± 0.37	1.0
	FIVβgluc	29.88 ± 0.87	21.69 ± 0.46	8.19 ± 0.99	−4.35 ± 0.99	20.30
Egr2 (X06746)	FIVMCS	22.35 ± 0.35	19.18 ± 0.18	3.17 ± 0.39	0.00 ± 0.39	1.0
	FIVβgluc	21.15 ± 0.51	21.69 ± 0.46	−0.54 ± 0.69	−3.71 ± 0.69	13.12

TaqMan chemistry was used to measure gene expression by means of real-time quantitative PCR (QPCR; *Materials and Methods*). A comparative C_T method allowed calculation of relative changes in gene expression of mice treated with FIVβgluc vs. FIVMCS. Glyceraldehyde-3-phosphate dehydrogenase (GAPDH) was used as a reference for all comparative analyses because microarray data revealed statistical consistency throughout experimental conditions and replicates. *t* tests on the replicates of each sample achieved $P < 0.001$ or better for every sample.

memory (38), was elevated approximately 10-fold by QPCR. *Egr2* is also important for peripheral nerve myelination (39). Expression of Cyr61, an extracellular matrix protein found in the human CNS, was shown to be induced on stimulation of m1 and m3 muscarinic acetylcholine receptors (40). We found a 3.8-fold increase in hippocampal Cyr61 mRNA.

Fe65 interacts with the γ-secretase-liberated tail of amyloid precursor protein (APP), and with the histone acetyltransferase Tip60 (41). Recent studies by Greengard and colleagues (42) showed that Fe65 also interacts with APP at the plasma membrane to foster axonal migration. In our studies, we noted significant elevations in Fe65 (Fig. 4*D* and Table 1). The role of Fe65 after FIVβgluc-mediated gene transfer is intriguing, and may imply enhanced neurite outgrowth and improved synaptic function. In support of this hypothesis, Sec8 expression was increased 9.6-fold (Fig. 4*D*). Sec8 is localized to regions of neurite outgrowth and is required for synaptogenesis (43).

Secondary elevations in lysosomal enzyme activity occurs in LSDs, and gene or enzyme therapy for the deficiency often normalizes these levels. For β-glucuronidase deficiency, enzyme replacement can reduce elevated α-galactosidase, β-galactosidase, and β-hexosaminidase levels (8, 11). It is currently unknown whether these secondary changes occur as a result of increased transcription or decreased protein degradation. We found that although reductions in RNA specific to β-hexosaminidase and α-galactosidase did not change greater than 2.5-fold, cathepsin L and α-mannosidase were significantly reduced (Fig. 4*D*). Whether this observation is reflective of the entire injected hemisphere, or only the harvested hippocampus, was not tested.

The combined results show that β-glucuronidase replacement reversed the severe neurological deficit in mice with established brain lysosomal storage disease. The data show that neuronal impairment has not occurred in aged MPS VII mice to a degree that function cannot be recovered. Before these studies, efficacy after gene, cell, or enzyme therapy to adult animal models with existing disease was assessed by clearance of the characteristic lysosomal distention observed within multiple cell types. We demonstrate that a functional assay of learning and memory is a more appropriate endpoint as we progress in the evaluation of vectors to treat human CNS disorders. Finally, our gene expression analyses using high-density oligonucleotide arrays and QPCR implied that β-glucuronidase treatment improved CNS function in manners beyond simple reconstitution of enzyme levels.

We thank Inês Martins, Qinwen Mao, Phil Sheridan, Kim Wahoski, and Christine McLennan for assistance, and Michael J. Welsh for critical discussions. This work was supported by National Institutes of Health Grants NS34568, DK54759, HD33531 (to B.L.D.), and MH57047 (to H.J.F.), and the Roy J. Carver Foundation (to B.L.D.).

1. Sly, W. S., Quinton, B. A., McAlister, W. H. & Rimoin, D. L. (1973) *J. Pediatr.* **82**, 249–257.
2. Birkenmeier, E. H., Davisson, M. T., Beamer, W. G., Ganschow, R. E., Vogler, C. A., Gwynn, B., Lyford, K. A., Maltais, L. M. & Wawrzyniak, C. J. (1989) *J. Clin. Invest.* **83**, 1258–1266.
3. Sands, M. S. & Birkenmeier, E. H. (1993) *Proc. Natl. Acad. Sci. USA* **90**, 6567–6571.
4. Ghodsi, A., Stein, C., Derksen, T., Yang, G., Anderson, R. D. & Davidson, B. L. (1998) *Hum. Gene Ther.* **9**, 2331–2340.
5. Stein, C. S., Ghodsi, A., Derksen, T. & Davidson, B. L. (1999) *J. Virol.* **73**, 3424–3429.
6. Ghodsi, A., Stein, C., Derksen, T., Martins, I., Anderson, R. D. & Davidson, B. L. (1999) *Exp. Neurol.* **160**, 109–116.
7. Daly, T. M., Vogler, C., Levy, B., Haskins, M. E. & Sands, M. S. (1999) *Proc. Natl. Acad. Sci. USA* **96**, 2296–2300.
8. Bosch, A., Perret, E., Desmaris, N., Trono, D. & Heard, J. M. (2000) *Hum. Gene Ther.* **11**, 1139–1150.
9. Snyder, E. Y., Taylor, R. M. & Wolfe, J. H. (1995) *Nature (London)* **374**, 367–370.
10. Lazarus, H. S., Sly, W. S., Kyle, J. W. & Hageman, G. S. (1993) *Exp. Eye Res.* **56**, 531–541.
11. Vogler, C., Sands, M., Higgins, A., Levy, B., Grubb, J., Birkenmeier, E. H. & Sly, W. S. (1993) *Pediatr. Res.* **34**, 837–840.
12. Birkenmeier, E. H., Barker, J. E., Vogler, C. A., Kyle, J. W., Sly, W. S., Gwynn, B., Levy, B. & Pegors, C. (1991) *Blood* **78**, 3081–3092.
13. O'Connor, L. H., Erway, L. C., Vogler, C. A., Sly, W. S., Nicholes, A., Grubb, J., Holmberg, S. W., Levy, B. & Sands, M. S. (1998) *J. Clin. Invest.* **101**, 1394–1400.
14. Sands, M. S., Vogler, C., Torrey, A., Levy, B., Gwynn, B., Grubb, J. & Sly, W. S. (1997) *J. Clin. Invest.* **99**, 1596–1605.
15. Frisella, W. A., O'Connor, L. H., Vogler, C. A., Roberts, M., Walkley, S., Levy, B., Daly, T. M. & Sands, M. S. (2001) *Mol. Ther.* **3**, 351–358.
16. Consiglio, A., Quattrini, A., Martino, S., Bensadoun, J. C., Dolcetta, D., Trojani, A., Benaglio, G., Marchesini, S., Cestari, V., Oliverio, A., *et al.* (2001) *Nat. Med.* **7**, 310–316.
17. Meikle, P. J., Hopwood, J. J., Clague, A. E. & Carey, W. F. (1999) *J. Am. Med. Assoc.* **281**, 249–254.
18. Skorupa, A. F., Fisher, K. J., Wilson, J. M., Parente, M. K. & Wolfe, J. H. (1999) *Exp. Neurol.* **160**, 17–27.
19. Franklin, K. B. J. & Paxinos, G. (1997) *The Mouse Brain in Stereotaxic Coordinates* (Academic, San Diego), pp. 1–190.
20. Johnston, J. C., Gasmi, M., Lim, L. E., Elder, J. H., Yee, J.-K., Jolly, D. J., Campbell, K. P., Davidson, B. L. & Sauter, S. L. (1999) *J. Virol.* **73**, 4991–5000.
21. Davidson, B. L., Doran, S. E., Shewach, D. S., Latta, J. M., Hartman, J. W. & Roessler, B. J. (1994) *Exp. Neurol.* **125**, 258–267.
22. Yee, J. K., Miyanohara, A., LaPorte, P., Bouic, K., Burns, J. C. & Friedman, T. (1994) *Proc. Natl. Acad. Sci. USA* **91**, 9564–9568.
23. Blömer, U., Naldini, L., Kafri, T., Trono, D., Verma, I. M. & Gage, F. H. (1997) *J. Virol.* **71**, 6641–6649.
24. Brooks, A. I., Cory-Slechta, D. A., Murg, S. M. & Federoff, H. J. (2000) *Neurobiol. Learn. Mem.* **74**, 241–258.
25. Brooks, A. I., Cory-Slechta, D. A., Bowers, W. J., Murg, S. L. & Federoff, H. J. (2000) *Hum. Gene Ther.* **11**, 2341–2352.
26. Brooks, A. I., Cory-Slecta, D. A. & Federoff, H. J. (2000) *Proc. Natl. Acad. Sci. USA* **97**, 13378–13383.
27. Tusher, V. G., Tibshirani, R. & Chu, G. (2001) *Proc. Natl. Acad. Sci. USA* **98**, 5116–5121.
28. PE Applied Biosystems (1997) *User Bulletin #2. ABI Prism 7700 Sequence Detection System*, Technical Notes (Perkin–Elmer, St. Pete Beach, FL), pp. 1–35.
29. Yamamoto, J. K., Hansen, H., Ho, E. W., Morishita, T. Y., Okuda, T., Sawa, T. R., Nakamura, R. M. & Pedersen, N. C. (1989) *J. Am. Vet. Med. Assoc.* **194**, 213–220.
30. Shacklett, B. L. & Luciw, P. A. (1994) *Virology* **204**, 860–867.
31. Tomonaga, K., Norimine, J., Shin, Y. S., Fukasawa, M., Miyazawa, T., Adachi, A., Toyosaki, T., Kawaguchi, Y., Kai, C. & Mikami, T. (1992) *J. Virol.* **66**, 6181–6185.
32. de Parseval, A. & Elder, J. H. (1999) *J. Virol.* **73**, 608–617.
33. Bastedo, L., Sands, M. S., Lambert, D. T., Pisa, M. A., Birkenmeier, E. & Chang, P. L. (1944) *J. Clin. Invest.* **94**, 1180–1186.
34. Hamilton, B. A., Smith, D. J., Mueller, K. L., Kerrebrock, A. W., Bronson, R. T., van Berkel, V., Daly, M. J., Kruglyak, L., Reeve, M. P., Nembauser, J. L., *et al.* (1997) *Neuron* **18**, 711–722.
35. Bustin, S. A. (2000) *J. Mol. Endocrinol.* **25**, 169–193.
36. Taubenfeld, S. M., Wiig, K. A., Monti, B., Dolan, B., Pollonini, G. & Alberini, C. M. (2001) *J. Neurosci.* **21**, 84–91.
37. Yukawa, K., Tanaka, T., Tsuji, S. & Akira, S. (1998) *J. Biol. Chem.* **273**, 31345–31351.
38. Pearse, D., Mirza, A. & Leah, J. (2001) *Brain Res.* **894**, 193–208.
39. Nagarajan, R., Svaren, J., Le, N., Araki, T. & Watson, M. (2001) *Neuron* **30**, 355–368.
40. Albrecht, C., von der Kammer, H., Mayhaus, M., Klauditny, J., Schweizer, M. & Nitsch, R. M. (2000) *J. Biol. Chem.* **275**, 28929–28936.
41. Cao, X. & Südhof, T. C. (2001) *Science* **293**, 115–120.
42. Sabo, S. L., Ikin, A. F., Buxbaum, J. D. & Greengard, P. (2001) *J. Cell Biol.* **153**, 1403–1414.
43. Hazuka, C. D., Foletti, D. L., Hsu, S. C., Kee, Y., Hopf, F. W. & Scheller, R. H. (1999) *J. Neurosci.* **19**, 1324–1334.

Commentary

Brain-directed gene therapy for lysosomal storage disease: Going well beyond the blood–brain barrier

William S. Sly*† and Carole Vogler‡

*Edward A. Doisy Department of Biochemistry and Molecular Biology, and ‡Department of Pathology, Saint Louis University School of Medicine, 1402 South Grand Boulevard, St. Louis, MO 63104

The lysosomal storage diseases (LSDs) are a heterogeneous group of disorders that affect 1/7,000 live-born infants, the majority of which develop central nervous system (CNS) disease. Brooks *et al.* (1) report exciting results from Davidson's group with brain-directed gene therapy for murine mucopolysaccharidosis (MPS) VII that are likely to have general implications for the treatment of CNS disease in LSD. Each LSD results from a deficiency of a single lysosomal enzyme important for degrading macromolecules that must be turned over in lysosomes. More than 40 LSDs have been described (2). Over the past two decades, dramatic progress has been made in understanding the biogenesis, structure, and function of lysosomes and the processes by which newly synthesized acid hydrolases are assembled, processed, and transported to lysosomes.

Understanding the receptors that target enzymes to lysosomes led to the development of successful enzyme replacement therapy.

Understanding the receptors that target enzymes to lysosomes, some of which are expressed on the cell surface, led to the development of successful enzyme replacement therapy for one of the LSDs, Gaucher Disease, a disorder of sphingolipid degradation (3). Gaucher Disease results from deficiency of glucocerebrosidase (β-glucosidase), the enzyme involved in the last step of sphingolipid degradation. Storage of glucocerebroside in macrophages produces tremendous enlargement of spleen and liver, disabling bone involvement and occasional pulmonary incapacity. The strategy for treatment involved purification of placental enzyme and later recombinant enzyme from Chinese hamster ovary cell secretions and modification of the native enzyme to expose mannose residues on oligosaccharides. This strategy targets the infused enzyme to the mannose receptors of fixed-tissue macrophages, precisely the cells affected by the storage; receptor-mediated endocytosis delivers enzyme to the lysosomes where the substrate is stored. Over 3,500 Gaucher Disease patients have been treated since the early 1990s, and the treatment is considered a clinical success (4). The major form of Gaucher Disease does not have CNS involvement. However, the less common neuropathic forms of Gaucher Disease will require a strategy for the enzyme to reach the CNS.

Another apparent success in the treatment of LSD is enzyme therapy for Fabry Disease, another sphingolipid disorder that does not produce lysosomal storage in the CNS (5). This LSD affects primarily vascular endothelial cells and results from a deficiency of α-galactosidase A, which leads to the pathological accumulation of globotriaosylceramide (GL3) and related glycosphingolipids in these cells. Kidney involvement leads to loss of renal function in the third or fourth decade of life. This disease does not affect brain directly, so enzyme access to brain is not required, but it does eventually lead to cerebral vascular insufficiency because of endothelial damage. Two clinical trials of enzyme produced by two different companies were reported recently (6, 7). Although both appear very promising, long-term data are not yet available. Both products have been approved for clinical use in Europe, and approval for both has been sought in the United States.

The MPS storage disorders are also moving up to the plate for enzyme replacement with clinical trials for MPS I (Hurler Disease, α-L-iduronidase deficiency) already reported (8), trials for MPS II (Hunter Disease, α-L-iduronidate sulfate deficiency) under way, and trials for MPS VI (Maroteaux–Lamy Disease, *N*-acetylgalactosamine-4-sulfatase deficiency) are just beginning. Although MPS VII (Sly Disease, β-glucuronidase deficiency) may be among the last of these disorders to be treated, it played an important role in the evolution of enzyme replacement therapy for the whole group of LSDs (9). Because it appears unlikely that infused lysosomal enzymes will cross the blood–brain barrier, there is not much optimism that i.v. administered enzyme alone will correct the CNS storage present in most of the MPS disorders.

Like the MPS, most of the other LSDs also have CNS involvement and therefore require a strategy for getting enzyme beyond the blood–brain barrier to achieve correction. A number of groups using a variety of viral vectors and enzyme-producing cells have achieved expression of enzyme in brain of animal models (10–17). Impressive degrees of clearing of local, and in some cases distant, storage have been demonstrated. These experiments raised hopes that arresting progression of CNS pathology was possible through brain-directed gene therapy. What few dared to hope was that this approach would not only prevent progression but also erase neurologic deficits. That is just what Davidson's group reports (1).

The authors (1) show that established CNS storage and the related functional deficits in MPS VII mice can be ameliorated by viral-mediated gene therapy. The lentivirus feline immunodeficiency viral vector they used transduced terminally differentiated cells in the brain and mediated β-glucuronidase (GUSB) gene transfer into CNS cells in adult MPS VII mice. This treatment resulted in secretion of GUSB from transduced cells and uptake by nontransduced cells, leading to reduction in preexisting established brain LSD. Correlating with the reduction in storage in the CNS, these adult mice with

See companion article on page 6216.

†To whom reprint requests should be addressed. E-mail: slyws@slu.edu.

www.pnas.org/cgi/doi/10.1073/pnas.102175599

established behavioral abnormalities related to the lysosomal storage had dramatic improvement in spatial learning and memory when GUSB was expressed. Finally, the correction of the pathology and cognitive improvement were accompanied by changes in expression of genes that have been associated with neuronal plasticity. These observations are particularly important because, as the authors point out, most patients with LSD are not diagnosed until they have established lysosomal storage lesions and functional defects. Recovery of function rather than protection from disease onset is a key goal for any effective therapy for human LSD, because most patients are diagnosed well after onset of CNS disease.

The model the authors (1) chose to study is murine MPS VII, the mouse model for human MPS VII or Sly Disease, which results from GUSB deficiency (18). MPS VII is one of the rarest of the human mucopolysaccharide storage disorders, each of which is produced by deficiency in one of the enzymes involved in the degradation of glycosaminoglycans (GAGs), formerly called mucopolysaccharides. Its importance in the evolution of our understanding of lysosomal enzyme targeting outweighs its clinical significance. When first discovered in the early 1970s, MPS VII had one unique feature among the MPS disorders: the deficient enzyme, GUSB, had been purified and characterized several years before the disease was identified. Addition of GUSB was shown to prevent and correct the accumulation of GAGs in fibroblasts from MPS VII patients (19, 20). Thus, MPS VII immediately attracted attention as a model to study enzyme replacement therapy. Studies of the cultured skin fibroblast model system led to the discovery that uptake of GUSB depends on cell surface receptors that recognize phosphate-containing sugar moieties (Man6-P) on the enzyme (21). The Man6-P residues are added to the GUSB and other acid hydrolases as a means of targeting intracellular enzymes

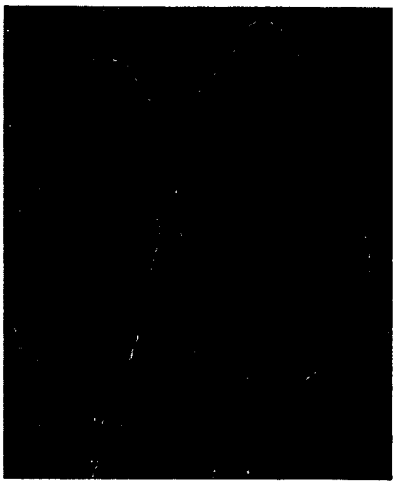

Fig. 1. An adult MPS VII (Sly Disease) mouse (*Left*) is much smaller than its phenotypically normal littermate (*Right*) and has facial dysmorphism with a broad shortened nose and short limbs.

to lysosomes. Another receptor was identified when injected GUSB, from which phosphate had been removed, was found to be rapidly taken up by fixed-tissue macrophage receptors that recognize exposed mannose residues (22). These studies paved the way for Brady and associates to develop "mannose-targeted" cerebrosidase for the treatment of Gaucher Disease (3, 4). These early findings naturally heightened hopes that enzyme replacement in MPS VII patients might lead to correction of lysosomal storage lesions in this disorder. However, MPS VII proved to be too rare (fewer than 100 cases recognized) and too variable to allow controlled experiments to evaluate the response to enzyme therapy.

Nonetheless, hopes for therapy for this and related disorders were greatly advanced by the discovery by Birkenmeier *et al.* at The Jackson Laboratory that GUSB deficiency in mice produces a disorder resembling Sly Disease in humans (23). (Fig. 1) MPS VII mice have a degenerative disease with progressive disability that reduces life span from an average of 28 to just 5 months. Progressive accumulation of undegraded glycosaminoglycans in lysosomes affects the spleen, liver, kidney, cornea, brain, heart valves, and skeletal system and produces widespread organ dysfunction. Progressive hearing loss leads to early deafness, and defects in learning and memory are evident (24–26).

The MPS VII mouse, with a well characterized and uniform genetic constitution and a relatively short life span, proved an attractive model to study experimental therapies for LSD. Mice with MPS VII responded well to bone marrow transplantation, although there was little reduction in brain storage vesicles (27, 28). Enzyme replacement using recombinant GUSB elicited dramatic improvements in visceral pathology but little change in the lysosomal storage lesions in brain unless given to newborns (29–32). Infused GUSB did not cross the blood–brain barrier in mice after 2 wk of age (32). Many promising studies have been reported recently by using this model to study gene therapy, including therapy for CNS storage (10–17). Brain-directed gene therapy, in which viral vectors were introduced directly into the brain, proved one way to bypass the blood–brain barrier, and several studies showed evidence of clearance of CNS storage. However, until now, none of these studies addressed the question raised by Brooks *et al.* (1): whether therapy that corrected the typical cellular pathology in brain could also erase preexisting neurological deficits. For this reason, the study by Davidson's group represents a major advance in this area.

Given the rapidly expanding number of animal models of LSD with CNS involvement and the generality of the biology of lysosomal enzyme transport, these studies are likely to be replicated in other animal models. If the results in other animal models turn out to be as promising as those presented for murine MPS VII, this study will likely be viewed as a landmark that took us well beyond the blood–brain barrier.

COMMENTARY

1. Brooks, A. I., Stein, C. S., Hughes, S. M., Heth, J., McCray, P. M., Jr., Sauter, S. L., Johnston, J. C., Cory-Slechta, D. A., Federoff, H. J. & Davidson, B. L. (2002) *Proc. Natl. Acad. Sci. USA* **99**, 6216–6221.
2. Scriver, C. R., Beaudet, A. L., Sly, W. S. & Valle, D., eds. (2001) *The Metabolic and Molecular Bases of Inherited Disease* (McGraw–Hill), 8th Ed., pp. 3371–3896.
3. Barton, N. W., Brady, R. O., Dambrosia, J. M., Di Bisceglie, A. M., Doppelt, S. H., Hill, S. C., Mankin, H. J., Murray, G. J., Parker, R. I. & Argoff, C. E. (1991) *N. Engl. J. Med.* **324**, 1464–1470.
4. Barranger, J. A. & O'Rourke, E. (2001) *J. Inherit. Metab. Dis.* **24** Suppl. 2, 89–96.
5. Desnick, R. J., Ioannou, Y. A. & Eng, C. M. (2001) in *The Metabolic and Molecular Bases of Inherited Disease*, eds, Scriver, C. R., Beaudet, A. L., Sly, W. S. & Valle, D. (McGraw–Hill), pp. 3733–3774.
6. Eng, C. M., Guffon, N., Wilcox, W. R., Germain, D. P., Lee, P., Waldek, S., Caplan, L., Linthorst, G. E. & Desnick, R. J. (2001) *N. Engl. J. Med.* **345**, 9–16.
7. Schiffmann, R., Kopp, J. B., Austin, H. A., III, Sabnis, S., Moore, D. F., Weibel, T., Balow, J. E. & Brady, R. O. (2001) *J. Am. Med. Assoc.* **285**, 2743–2749.
8. Kakkis, E. D., Muenzer, J., Tiller, G. E., Waber, L. Belmont, J., Passage, M., Izykowski, B., Phillips, J., Doroshow, R., Walot, I., *et al.* (2001) *N. Engl. J. Med.* **344**, 182–188.
9. Sly, W. S. (1993) *Nat. Genet.* **4**, 105–106.
10. Frisella, W. A., O'Connor, L. H., Vogler, C. A., Roberts, M., Walkley, S., Levy, B., Daly, T. M. & Sands, M. S. (2001) *Mol. Ther.* **3**, 351–358.
11. Ghodsi, A., Stein, C., Derksen, T., Martins, I., Anderson, R. D. & Davidson, B. L. (1999) *Exp. Neurol.* **160**, 109–116.
12. Ohashi, T., Watabe, K., Uehara, K., Sly, W. S., Vogler, C. & Eto, Y. (1997) *Proc. Natl. Acad. Sci. USA* **94**, 1287–1292.
13. Snyder, E. Y., Taylor, R. M. & Wolfe, J. H. (1995) *Nature (London)* **374**, 367–370.
14. Watson, G. L., Sayles, J. N., Chen, C., Elliger, S. S., Elliger, C. A., Raju, N. R., Kurtzman, G. J. & Podsakoff, G. M. (1998) *Gene Ther.* **5**, 1642–1649.
15. Bosch, A., Perret, E., Desmaris, N. & Heard, J. M. (2000) *Mol. Ther.* **1**, 63–70.
16. Bosch, A., Perret, E., Desmaris, N., Trono, D. & Heard, J. M. (2000) *Hum. Gene Ther.* **20**, 1139–1150.
17. Xia, H., Mao, Q. & Davidson, B. L. (2001) *Nat. Biotechnol.* **19**, 640–644.

18. Sly, W. S., Quinton, B. A., McAlister, W. H. & Rimoin, D. L. (1973) *J. Pediatr.* **82**, 249–257.
19. Hall, C. W., Cantz, M. & Neufeld, E. F. (1973) *Arch. Biochem. Biophys.* **155**, 32–38.
20. Brot, F. E., Glaser, J. H., Roozen, K. J., Sly, W. S. & Stahl, P. D. (1974) *Biochem. Biophys. Res. Commun.* **57**, 1–8.
21. Kaplan, A., Achord, D. T. & Sly, W. S. (1977) *Proc. Natl. Acad. Sci. USA* **74**, 2026–2030.
22. Achord, D. T., Brot, F. E., Bell, C. E. & Sly, W. S. (1978) *Cell* **15**, 269–278.
23. Birkenmeier, E. H., Davisson, M. T., Beamer, W. G., Ganschow, R. E., Vogler, C. A., Gwynn, B., Lyford, K. A., Maltais, L. M. & Wawrzyniak, C. J. (1989) *J. Clin. Invest.* **83**, 1258–1266.
24. Berry, C. L., Vogler, C., Galvin, N. J., Birkenmeier, E. H. & Sly, W. S. (1994) *Lab. Invest.* **71**, 438–445.
25. Chang, P. L., Lambert, D. T. & Pisa, M. A. (1993) *NeuroReport* **4**, 507–510.
26. O'Connor, L. H., Erway, L. C., Vogler, C. A., Sly, W. S., Nicholes, A., Grubb, J., Holmberg, S. W., Levy, B. & Sands, M. S. (1998) *J. Clin. Invest.* **101**, 1394–1400.
27. Birkenmeier, E. H., Barker, J. E., Vogler, C. A., Kyle, J. W., Sly, W. S., Gwynn, B., Levy, B. & Pegors, C. (1991) *Blood* **78**, 3081–3092.
28. Sands, M. S., Erway, L. C., Vogler, C., Sly, W. S. & Birkenmeier, E. H. (1995) *Blood* **86**, 2033–2040.
29. Sands, M. S., Vogler, C., Kyle, J. W., Grubb, J. H., Levy, B., Galvin, N., Sly, W. S. & Birkenmeier, E. H. (1994) *J. Clin. Invest.* **93**, 2324–2331.
30. Sands, M. S., Vogler, C., Torrey, A., Levy, B., Gwynn, B., Grubb, J., Sly, W. S. & Birkenmeier, E. H. (1997) *J. Clin. Invest.* **99**, 1596–1605.
31. Vogler, C., Sands, M. S., Levy, B., Galvin, N., Birkenmeier, E. H. & Sly, W. S. (1996) *Pediatr. Res.* **39**, 1050–1054.
32. Vogler, C., Levy, B., Galvin, N. J., Thorpe, C., Sands, M. S., Barker, J. E., Baty, J., Birkenmeier, E. H. & Sly, W. S. (1999) *Pediatr. Res.* **45**, 838–844.

NCBI

PubMed

National Library of Medicine NLM

Entrez PubMed Nucleotide Protein Genome Structure PMC Journals Books

Search PubMed for Go Clear

Limits Preview/Index History Clipboard Details

About Entrez

Display Abstract Show: 20 Sort Send to Text

Text Version

Entrez PubMed
Overview
Help | FAQ
Tutorial
New/Noteworthy
E-Utilities

PubMed Services
Journals Database
MeSH Database
Single Citation Matcher
Batch Citation Matcher
Clinical Queries
LinkOut
Cubby

Related Resources
Order Documents
NLM Gateway
TOXNET
Consumer Health
Clinical Alerts
ClinicalTrials.gov
PubMed Central

Privacy Policy

1: Hum Gene Ther. 2002 Mar 20; 13(5): 665-74.

Related Articles, Links

ingenta select

Highly efficient and specific gene transfer to Purkinje cells in vivo using a herpes simplex virus I amplicon.

Agudo M, Trejo JL, Lim F, Avila J, Torres-Aleman I, Diaz-Nido J, Wandosell F.

Centro de Biologia Molecular Severo Ochoa CSIC-UAM, Universidad Autonoma de Madrid, Madrid 28049, Spain.

The transduction of cerebellar neurons in vivo with herpes simplex virus 1 (HSV-1) amplicon carrying the lacZ gene has been investigated after injection of the vector in the cerebellar cortex, ventricles, and inferior olive of adult rats. Injection into the cerebellar cortex resulted in transduction of Purkinje cells near the needle tract and injection into the ventricles yielded no transduced neurons. In contrast, high transduction efficiency was achieved by vector injection into the inferior olive, resulting in one of three positive Purkinje cells all over the ipsilateral and contralateral cerebellar hemispheres. Because neurons in the deep cerebellar nuclei are also transduced, we suggest that the vector is delivered from the inferior olive to the cerebellar nuclei and then to Purkinje cells by retrograde axonal transport. Expression of the lacZ gene within Purkinje cells was surprisingly persistent and was maintained at the same level for at least 40 days. Importantly, no signs of either toxicity or inflammation were observed in the cerebellum after vector injection, except for the borders of the needle tract where some reactive astrocytes were detected. Indeed, motor coordination of treated animals was entirely normal, as assessed by the rota-rod test. These results demonstrate that HSV-1 amplicon vectors can effect safe and stable transgene expression in Purkinje cells in vivo, raising the possibility of using these vectors for long-term gene therapy of human cerebellar disorders.

PMID: 11916489 [PubMed - indexed for MEDLINE]

Display Abstract Show: 20 Sort Send to Text

Write to the Help Desk
NCBI | NLM | NIH
Department of Health & Human Services
Freedom of Information Act | Disclaimer

Jan 20 2004 07:12:30

NCBI PubMed National Library of Medicine NLM

Entrez PubMed Nucleotide Protein Genome Structure PMC Journals Books

Search PubMed for Go Clear

Limits Preview/Index History Clipboard Details

About Entrez

Display Abstract Show: 20 Sort Send to Text

Text Version

Entrez PubMed
Overview
Help | FAQ
Tutorial
New/Noteworthy
E-Utilities

PubMed Services
Journals Database
MeSH Database
Single Citation Matcher
Batch Citation Matcher
Clinical Queries
LinkOut
Cubby

Related Resources
Order Documents
NLM Gateway
TOXNET
Consumer Health
Clinical Alerts
ClinicalTrials.gov
PubMed Central

Privacy Policy

1: Brain Res Mol Brain Res. 2003 Nov 6; 119(1): 1-9.

Related Articles, Links

ELSEVIER FULL-TEXT ARTICLE

Systemic FIV vector administration: transduction of CNS immune cells and Purkinje neurons.

Kyrkanides S, Miller JH, Federoff HJ.

Department of Dentistry, School of Medicine and Dentistry, University of Rochester, Rochester, NY, USA. stephanos_Kyrkanides@urmc.rochester.edu

The systemic effects of gene therapy have been previously described in a variety of peripheral organs following intravenous administration or intraperitoneal inoculation of viral vectors, as well as in the brain following intracranial administration. However, limited information is available on the ability of viral vectors to cross the blood-brain barrier and infect cells located within the central nervous system (CNS). We employed a VSV-G pseudotyped FIV(lacZ) vector capable of transducing dividing, growth-arrested, as well as post-mitotic cells with the reporter gene lacZ. Adult mice were injected intraperitoneally with FIV(lacZ), and the expression of beta-galactosidase was studied 5 weeks following treatment in the brain, liver, spleen and kidney by X-gal histochemistry and immunocytochemistry. Interestingly, relatively low doses of FIV(lacZ) administered intraperitoneally lead to beta-galactosidase detection in the brain and cerebellum. The identity of these cells was confirmed by double immunofluorescence, and included CD31-, CD3- and CD11b-positive cells. Fluorescent microspheres co-injected with FIV(lacZ) virus were identified within mononuclear cells in the brain parenchyma, suggesting infiltration of peripheral immune cells in the CNS. Cerebellar Purkinje neurons were also transduced in all adult-injected mice. Our observations indicate that relatively low doses of FIV(lacZ) administered intraperitoneally resulted in the transduction of immune cells in the brain, as well as a specific subset of cerebellar neurons.

PMID: 14597224 [PubMed - in process]

Display Abstract Show: 20 Sort Send to Text

Write to the Help Desk
NCBI | NLM | NIH
Department of Health & Human Services
Freedom of Information Act | Disclaimer

Jan 20 2004 07:12:30

NCBI PubMed National Library of Medicine

Entrez PubMed Nucleotide Protein Genome Structure PMC Journals Books

Search PubMed for Go Clear

Limits Preview/Index History Clipboard Details

About Entrez

Display Abstract Show: 20 Sort Send to Text

Text Version

Entrez PubMed
Overview
Help | FAQ
Tutorial
New/Noteworthy
E-Utilities

PubMed Services
Journals Database
MeSH Database
Single Citation Matcher
Batch Citation Matcher
Clinical Queries
LinkOut
Cubby

Related Resources
Order Documents
NLM Gateway
TOXNET
Consumer Health
Clinical Alerts
ClinicalTrials.gov
PubMed Central

Privacy Policy

1: Gene Ther. 2000 May; 7(9): 759-63.

Related Articles, Links

nature publishing group

Widespread gene transfection into the central nervous system of primates.

Hagihara Y, Saitoh Y, Kaneda Y, Kohmura E, Yoshimine T.

Department of Neurosurgery, Osaka University Graduate School of Medicine, 2-2 Yamadaoka, Suita, Osaka 565-0871, Japan.

We attempted in vivo gene transfection into the central nervous system (CNS) of non-human primates using the hemagglutinating virus of Japan (HVJ)-AVE liposome, a newly constructed anionic type liposome with a lipid composition similar to that of HIV envelopes and coated by the fusogenic envelope proteins of inactivated HVJ. HVJ-AVE liposomes containing the lacZ gene were applied intrathecally through the cisterna magna of Japanese macaques. Widespread transgene expression was observed mainly in the neurons. The lacZ gene was highly expressed in the medial temporal lobe, brainstem, Purkinje cells of cerebellar vermis and upper cervical cord (29.0 to 59.4% of neurons). Intrastriatal injection of an HVJ-AVE liposome-lacZ complex made a focal transfection around the injection sites up to 15 mm. We conclude that the infusion of HVJ-AVE liposomes into the cerebrospinal fluid (CSF) space is applicable for widespread gene delivery into the CNS of large animals. Gene Therapy (2000) 7, 759-763.

PMID: 10822302 [PubMed - indexed for MEDLINE]

Display Abstract Show: 20 Sort Send to Text

Write to the Help Desk
NCBI | NLM | NIH
Department of Health & Human Services
Freedom of Information Act | Disclaimer

Jan 20 2004 07:12:30

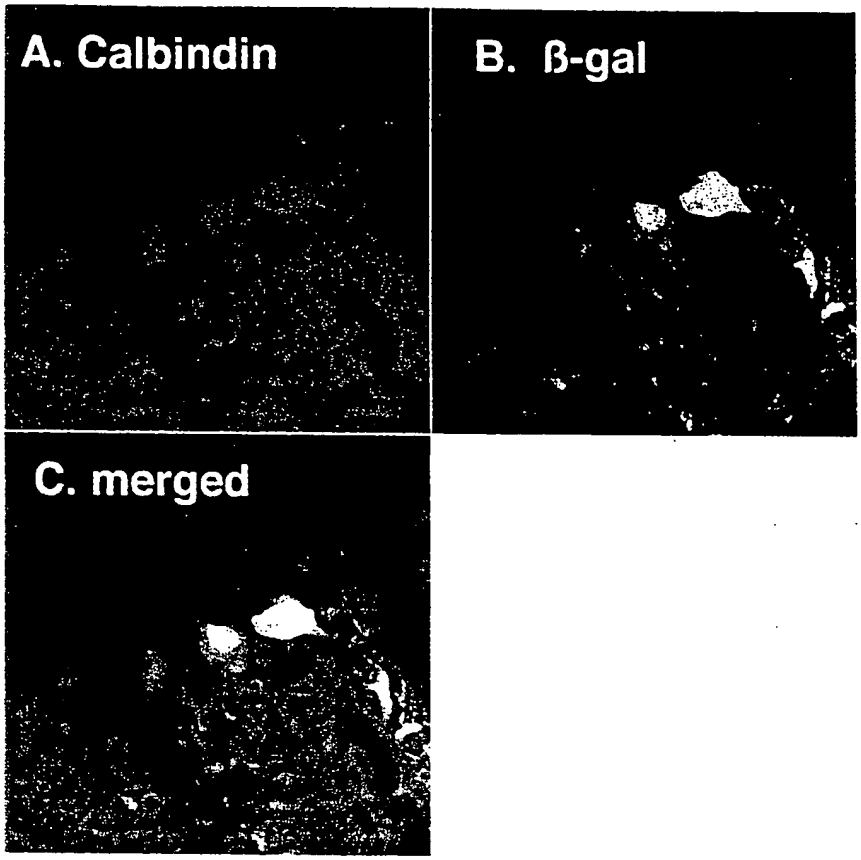

FIG. 3. Dual immunofluorescent staining for β-galactosidase and Purkinje cells. FIVβgal was injected into a cerebellar lobule of a mouse brain. Six weeks later, 50-μm coronal brain sections were dual stained with a calbindin-specific antibody (A, calbindin, red fluorescence), to detect the calbindin positive Purkinje neurons, and a β-galactosidase-specific antibody (B, β-gal, green fluorescence) to detect FIVβgal-transduced cells. Overlapping red and green fluorescence appears yellow in the merged images (C) and identifies β-galactosidase-expressing transduced Purkinje cells.

tissue section. This allows the user to unambiguously determine whether the signals from two different fluorochromes are arising from the same cell. Collection of a series of emission data from top to bottom of the tissue section allows for three-dimensional reconstruction and morphological assessment of the stained cells. Procedures for use of a confocal microscope and analysis of the data vary with the microscope and associated software.

When tissues are dual stained with one antibody that is FITC- or Alexa 488-conjugated (green fluorescence) and another that is rhodamine or CY-3-conjugated (red fluorescence), colocalization of signals appears yellow. Figure 2 shows colocalization of β-galactosidase and the neuronal cell marker NeuN in striatal neurons. Figure 3 shows colocalization of β-galactosidase and calbindin in cerebellar Purkinje cells.

Concluding Remarks

Gene transfer to the CNS for the treatment of neurodegenerative diseases is gradually progressing toward clinical application, as development of vectors advances. Successful therapy will ultimately depend on the use of a suitable vector and an effective therapeutic transgene. FIV-based vectors mediate stable gene transfer to cerebral neurons and cerebellar Purkinje cells and provide a sound basis for the further design of vectors applicable to human CNS disorders.

Acknowledgments

The authors thank our collaborators previously of Chiron Technologies, Center for Gene Therapy (Sybille Sauter, Julie Johnston, Phil Sheridan, Day Townsend, Tom Dubensky, and Doug Jolly) for development of the FIV constructs and vector production system, and for their scientific contribution. For technical support we thank Stephanie Hughes, Inês Martins, and The University of Iowa Gene Transfer Vector Core (Patrick Staber) and Cell Morphology Core. We thank Joe Alisky for critical comments and technical contributions, and Christine McLennan for manuscript preparation. These protocols were developed with support from the NIH (NS34568, HD33531, DK54759) and the Roy J. Carver Trust.

[25] Gene Transfer to the Brain Using Feline Immunodeficiency Virus-Based Lentivirus Vectors

By COLLEEN S. STEIN and BEVERLY L. DAVIDSON

Introduction

Neurodegenerative diseases of the central nervous system (CNS) can display restricted or widespread CNS pathology. Examples of disorders demonstrating extensive CNS involvement include Alzheimer's disease,[1] the neuronal ceroid lipofuscinoses (CLN or NCL),[2,3] and the mucopolysaccharidoses (MPS types I to VII).[4] Disorders with relatively restricted neuronal cell loss include Parkinson's disease[5] and motor neuron diseases such as amyotrophic lateral sclerosis (ALS)[6] and the spinocerebellar ataxias (SCA).[7] For many neurodegenerative diseases, gene therapy approaches are being investigated, and may prove viable treatment options. Studies in our own laboratory include investigation of CNS gene transfer strategies for treatment of CLN, MPS, ALS, and the SCA. The CLN and MPS are inherited lysosomal storage diseases characterized by abnormal lysosomal storage deposits. CNS manifestations of these diseases include advancing neuronal dysfunction resulting in progressive cognitive and visual deterioration. ALS is characterized by degeneration of motor neurons in the spinal cord and brain stem, followed by further degeneration of corticospinal neurons in the cerebral cortex. ALS patients manifest increasingly severe muscular weakness and eventual death due to neuromuscular respiratory failure. Approximately 5% of ALS is caused by mutations in superoxide dismutase (SOD1) while 95% are of unknown origin. The SCA are inherited disorders characterized by selective loss of cerebellar neurons leading to motor dysfunction and ataxia.

Gene transfer strategies are often based on delivery of a correct cDNA copy of the affected gene to the relevant cells *in vivo*. For many of the lysosomal storage diseases, the affected gene encodes a soluble lysosomal protein that when overexpressed can be secreted and taken up by neighboring cells via mannose or

[1] E. Braak, K. Griffing, K. Arai, J. Bohl, H. Bratzke, and H. Braak, *Eur. Arch. Psychiatry Clin. Neurosci.* **249,** 14 (1999).
[2] L. Peltonen, M. Savukoski, and J. Vesa, *Curr. Opin. Genet. Dev.* **10,** 299 (2000).
[3] M. J. Bennett and S. L. Hofmann, *J. Inherit. Metab. Dis.* **22,** 535 (1999).
[4] E. F. Neufeld and J. Muenzer, *in* "The Metabolic and Molecular Bases of Inherited Disease" (C. R. Scriver, A. L. Beaudet, W. S. Sly, and D. Valle, eds.), p. 2465. McGraw-Hill, New York, 1995.
[5] M. C. Bohn, *Mol. Ther.* **1,** 494 (2000).
[6] L. J. Martin, A. C. Price, A. Kaiser, A. Y. Shaikh, and Z. Liu, *Int. J. Mol. Med.* **5,** 3 (2000).
[7] H. Y. Zoghbi and H. T. Orr, *Annu. Rev. Neurosci.* **23,** 217 (2000).

mannose 6-phospate receptors. As a result, transduction of a small proportion of CNS cells can potentially mediate widespread correction. The task is more difficult with a membrane-integral lysosomal protein, where prevention and/or reversal of neurodegeneration may necessitate delivery of the gene to most affected CNS cells.

In instances where the defective protein performs a dominant negative function, or deleterious function, provision of a normal version of the gene may be without beneficial effect. Several of the SCA fall into this category; expanded polyglutamine tracts create a toxic gain of function in the encoded protein.[7] Similarly the SOD1 mutation in ALS is a gain of function mutation leading to accumulation of toxic reactive metabolites.[6] Gene transfer approaches for such disorders are aimed at either down-regulating expression of the mutated gene or countering its toxic effects. Neuroprotective strategies such as transfer of genes expressing neurotrophic factors or anti-apoptotic molecules could be undertaken to prevent or delay neuronal cell death, and may find general application to neurodegenerative diseases.[8–13]

Targeting of neurons requires use of a vector that can transduce fully differentiated nondividing cells. *In vivo* rodent studies have found that although recombinant adenoviruses based on serotype 5 can infect neurons *in vivo,* their preference is for astrocytes,[14–16] and the vector-associated inflammatory response often curtails transgene expression.[15,17] Commonly used retroviral vectors based on oncoretroviruses show strict requirements for cell division,[18] and thus are not be useful for targeting neurons. Retroviral vectors based on lentiviruses, such as human immunodeficiency virus (HIV) or feline immunodeficiency virus (FIV), possess nuclear import mechanisms and demonstrate ability to transduce nondividing, fully

[8] D. L. Choi-Lundberg, Q. Lin, Y.-N. Chang, C. M. Hay, H. Mohajeri, and B. L. Davidson, *Science* **275,** 838 (1997).

[9] J. H. Kordower, M. E. Emborg, J. Bloch, S. Y. Ma, Y. Chu, L. Leventhal, J. McBride, E. Y. Chen, S. Palfi, B. Z. Roitberg, W. D. Brown, J. E. Holden, R. Pysalski, M. D. Taylor, P. Carvey, Z. Ling, D. Trono, P. Hantraye, N. Déglon, and P. Aebisher, *Science* **290,** 767 (2000).

[10] D. L. Choi-Lundberg and M. C. Bohn, *in* "Stem Cell Biology and Gene Therapy" (P. J. Quesenberry, G. S. Stein, B. Forget, and S. Weissman, eds.), John Wiley & Sons, New York, 1996.

[11] M. Caleo, M. C. Cenni, E. Menna, M. Costa, L. Zentilin, and M. Giacca, *Proc. Soc. Neurosci.* **1,** 122.11 (abstract) (2000).

[12] R. Dalal, F. E. Samson, and Z. Suo, *Proc. Soc. Neuroscience* **1,** 307.8 (abstract) (2000).

[13] M. Yamada, T. Oligino, M. Mata, J. R. Goss, J. C. Glorioso, and D. J. Fink, *Proc. Natl. Acad. Sci. U.S.A.* **96,** 4078 (1999).

[14] J. M. Alisky, S. M. Hughes, S. L. Sauter, J. M. Alisky, S. M. Hughes, S. L. Sauter, D. J. Jolly, T. W. Dubensky, P. D. Staber, J. A. Chiorini, and B. L. Davidson, *NeuroReport* **11,** 2669 (2000).

[15] U. Blömer, L. Naldini, T. Kafri, D. Trono, I. M. Verma, and F. H. Gage, *J. Virol.* **71,** 6641 (1997).

[16] K. Moriyoshi, L. J. Richards, C. Akazawa, D. D. M. O'Leary, and S. Nakanishi, *Neuron* **16,** 255 (1996).

[17] K. Kajiwara, A. P. Byrnes, H. M. Charlton, M. J. Wood, and K. J. Wood, *Hum. Gene Ther.* **8,** 253 (1997).

[18] P. F. Lewis and M. Emerman, *J. Virol.* **68,** 510 (1994).

differentiated cell types including postmitotic neurons, *in vitro* and *in vivo*.[15,19–21] Lentiviral vector gene transfer to the brain is accompanied by minimal if any vector-associated inflammatory response, and transgene expression is stable.[15] Thus lentivirus-based vectors show promise for neuronal gene transfer. Our recent studies have investigated the use of recombinant FIV-based vectors for direct gene transfer to the MPS VII mouse brain cerebrum[22] as a model for gene therapy application for widespread neurodegenerative diseases. We have also investigated the feasibility of recombinant FIV as a vector for gene transfer to cerebellar neurons,[14] for potential therapeutic use in degenerative diseases of the cerebellum.

Wild-type FIV causes an immunodeficiency disease in cats and, despite prevalent exposure, is not known to cause infection or disease in humans.[23] Like other retroviruses, FIV is an enveloped virus, with a single stranded RNA genome. Cell entry of enveloped viruses is a fusogenic process directed by the virus envelope protein, resulting in delivery of nucleocapsids either directly into the cytoplasm or into intracellular vesicular compartments. Reverse transcription, mediated by the retroviral enzyme reverse transcriptase (RT), then proceeds to generate double-stranded DNA. In oncoretroviruses, such as the Moloney murine leukemia virus (MLV, used commonly in recombinant form as a gene transfer vector), access of the double-stranded DNA preintegration complex to the host cell genome requires dissolution of the nuclear membrane, as occurs during cell mitosis. In contrast, lentiviral preintegration complexes are equipped to mediate nuclear import, thus enabling integration of genetic material into the genomes of nondividing as well as dividing cells.

The native FIV genome contains the basic retroviral *gag, pol,* and *env* open reading frames (Fig. 1A) for production of matrix and nucleocapsid proteins, RT, polymerase and integrase proteins, and envelope proteins, respectively.[24] The FIV genome is simpler than the HIV genome, and encodes only three accessory proteins: vif, orf2, and rev.[25] Reports by Poeschla *et al.*,[20] Johnston *et al.*,[19] and Curran *et al.*[26] describe construction of recombinant FIV gene transfer vectors that can be produced at high particle titer and are able to efficiently transduce dividing and nondividing cells. These protocols utilize a triple plasmid transfection system. The packaging plasmid provides all the necessary viral proteins in

[19] J. C. Johnston, M. Gasmi, L. E. Lim, J. H. Elder, J. K. Yee, D. J. Jolly, K. P. Campbell, B. L. Davidson, and S. L. Sauter, *J. Virol.* **73,** 4991 (1999).

[20] E. M. Poeschla, F. Wong-Staal, and D. J. Looney, *Nat. Med.* **4,** 354 (1998).

[21] G. Wang, V. Slepushkin, and J. Zabner, *J. Clin. Invest.* **104,** R55 (1999).

[22] C. S. Stein, A. I. Brooks, J. A. Heth, T. W. Dubensky, Jr., S. L. Sauter, K. Townsend, D. A. Cory-Slechta, M. A. Howard, H. J. Federoff, and B. L. Davidson, *Proc. Soc. Neurosci.* **1,** 668.7 (2000).

[23] J. K. Yamamoto, H. Hansen, E. W. Ho, T. Y. Morishita, T. Okuda, T. R. Sawa, R. M. Nakamura, and N. C. Pedersen, *J. Am. Vet. Med. Assoc.* **194,** 213 (1989).

[24] T. Miyazawa, K. Tomonaga, Y. Kawaguchi, and T. Mikami, *Arch. Virol.* **134,** 221 (1994).

[25] K. Tomonaga and T. Mikami, *J. Gen. Virol.* **77,** 1611 (1996).

[26] M. A. Curran, S. M. Kaiser, P. L. Achacoso, and G. P. Nolan, *Mol. Ther.* **1,** 31 (2000).

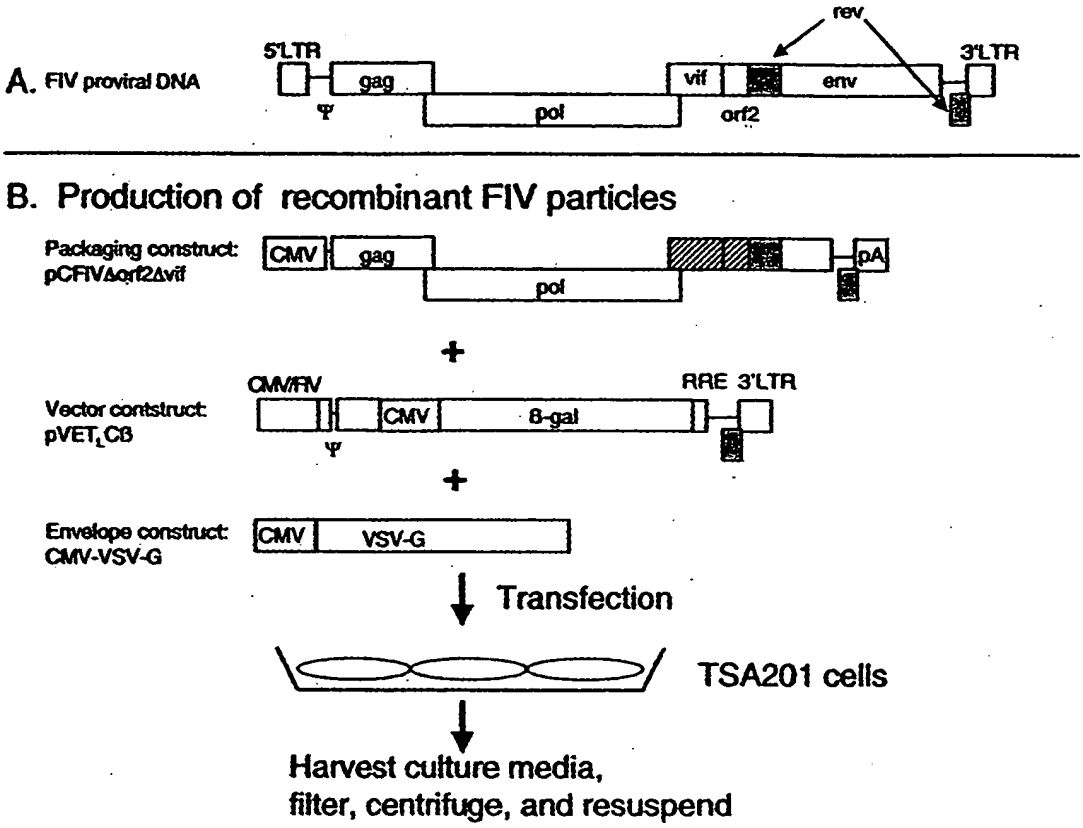

FIG. 1. Recombinant FIV particle production. (A) FIV proviral DNA contains three large open reading frames (*gag, pol,* and *env*), and three small regions encoding accessory proteins (*vif, orf2,* and *rev*). The packaging signal (Ψ) extents from noncoding sequences just downstream of the 5′ LTR to coding sequences within the 5′ portion of *gag*. (B) For particle production, TSA201 cells are transfected with packaging, vector, and envelope plasmids. Full-length transcripts from the vector plasmid contain an intact packaging signal and are packaged into enveloped particles. At 24, 36, and 72 h posttransfection the culture media (containing particles) is harvested and filtered, and the particles are concentrated by centrifugation.

trans (except for the env protein), but it is not packaged into particles. The vector plasmid contains the transgene expression cassette and retains the minimal *cis*-acting viral sequences to allow efficient genome packaging, reverse transcription, and integration. The third plasmid encodes a chosen envelope protein in *trans*. Most lentiviral vector studies to date have used recombinant vectors pseudotyped with the envelope glycoprotein from vescicular stomatitis virus (VSV-G), because it imparts particle stability and mediates widespread cellular tropism.[27] This chapter outlines techniques for (1) production of VSV-G-pseudotyped recombinant FIV particles encoding the reporter protein bacterial β-galactosidase (FIVβgal), (2) vector injection in mouse brain striatum and cerebellum, and (3) immunofluorescent staining for determination of cell types transduced.

[27] J. C. Burns, T. Friedmann, W. Driever, M. Burrascano, and J. K. Yee, *Proc. Natl. Acad. Sci. U.S.A.* **90,** 8033 (1993).

Materials

Recombinant FIV Particle Production

Plasmids: packaging construct, vector construct, and envelope construct (Fig. 1B): The FIV packaging construct (pCFIVΔorf2Δvif)[19] was derived from the FIV molecular clone p34TF10. The packaging construct retains full-length *gag* and *pol*, and *rev*, but contains a deletion in the *env* gene, and mutations in *vif* and *orf2* genes. The vif and orf2 accessory proteins have been determined to be dispensable both for recombinant particle production and for transduction of brain *in vivo*. The third accessory gene, *rev*, is retained since rev is necessary for efficient nuclear export of long and full-length transcripts. The native 5′ LTR has been replaced by the human cytomegalovirus (CMV) immediate early promoter/enhancer, and the 3′ LTR has been replaced with the simian virus 40 polyadenylation signal. The vector construct ($pVET_LC\beta$)[19] carries the transgene of interest driven by an internal promoter. Here the *lacz* gene, encoding the reporter protein bacterial β-galactosidase, is driven by the CMV promoter. The 5′ U3 of FIV has been replaced with the CMV promoter. $pVET_LC\beta$ has been deleted of all viral coding regions with the exception of a 5′ portion of *gag* (which contains part of the packaging signal). Last a third plasmid, the envelope construct, provides the envelope protein in trans. Here we use a plasmid encoding the VSV-G directed by the CMV promoter.[28]

TSA201 cells[29] maintained in exponential growth in DMEM-10. TSA201 cells were derived from 293 human embryonic kidney epithelial cells (ATCC CRL-1573) and grow as monolayers. They are easily lifted with trypsin for passage.

Incubator at 37° with 5% CO_2

HEPES buffered saline (HBS):

HEPES	5.0 g
NaCl	8.0 g
KCl	0.37 g
$Na_2HPO_4 \cdot 7H_2O$	0.188 g
Glucose	1.0 g

Bring to 1 liter in ddH_2O, pH to 7.1 with concentrated NaOH, filter sterilize and store at 4°

2.5 *M* $CaCl_2$

DMEM: Dulbecco's modified Eagle's medium

DMEM-10: DMEM with 10% fetal calf serum, 100 U/ml penicillin, and 100 μg/ml streptomycin

[28] J.-K. Yee, T. Friedmann, and J. C. Burns, *In* "Methods in Cell Biology," Vol. 43, p. 99. Academic Press, San Diego, 1994.

[29] E. S. Shen, G. M. Cooke, and R. A. Horlick, *Gene* **156**, 235 (1995).

DMEM-2: DMEM with 2% fetal bovine serum, 100 U/ml penicillin, and 100 μg/ml streptomycin
Bottle-top filters (500 ml capacity, Nalgene PES low protein binding)
Lactose buffer: phosphate-buffered saline (PBS), pH 7.4 (Sigma P-3813) with 40 mg/ml lactose, filter-sterilized
Sorvall centrifuge RC 26 Plus, with SLA 1500 rotor
Sorvall centrifugation bottles (250 ml capacity)

Determination of Transduction Titer by X-Gal Staining

HT-1080 cells (ATCC CRL-121) maintained in exponential growth in DMEM-10. These cells are derived from human fibrosarcoma and grow as monolayers. They are easily lifted with trypsin for passage.

Incubator at 37° with 5% CO_2
Six-well tissue culture dishes
DMEM-2 and DMEM-10 (see above)
Polybrene stock: 8 mg/ml in ddH_2O, filter sterilized
DMEM-2/Polybrene: On the day of use, dilute the Polybrene stock 1/2000 in DMEM-2, for a final Polybrene concentration of 4 μg/ml
Dilution tubes (3.5 ml polystyrene sterile tubes)
1% glutaraldehyde in PBS
KC Mixer:

35 m*M* K_3 Fe(CN)$_6$	5.74 g
35 m*M* K_4 Fe(CN)$_6$ · 3HO	7.35 g
2 m*M* $MgCl_2$	1 ml of 1 *M* stock
0.01% sodium desoxycholate	0.5 ml of 10% stock
0.02% NP40	1.0 ml of 10% stock

Add to PBS for a final volume of 500 ml. Do not add the $MgCl_2$ until the previous ingredients have dissolved. Filter through a 0.45 μm bottle top filter and store in the dark at 4°.

X-Gal (5′-bromo-4-chloro-3-indolyl-β-D-galactopyranoside) stock: Dissolve at 40 mg/ml in *N*′,*N*-dimethyl formamide, and store at −20° (does not freeze).

X-Gal solution (staining solution): Dilute X-Gal stock to 1 mg/ml in the KC mixer just prior to use. Prewarming separately the KC mixer and the X-Gal stock at 37° before mixing can help to avoid precipitation that can occur with longer incubation times.

Vector Injection into Adult Mouse Striatum or Cerebellum

Ketamine/xylazine mix: combine 8.9 ml of sterile PBS with 1 ml of 100 mg/ml ketamine and 0.1 ml of 100 mg/ml xylazine for final concentrations of 10 mg/ml ketamine and 1 mg/ml xylazine.

Insulin syringe with attached 28-gauge needle
Underpads (blue chucks)
Eye ointment (bacitracin zinc and polymyxin B sulfate ophthalmic ointment)
Razor to shave mouse head
Iodine tincture
Surgical instruments (autoclaved): scalpel and blades, curette, forceps, scissors, hemostat
Dry sterilizer (Germinator 500, Cellpoint Scientific, Inc.)
Small sterile beaker with 70% ethanol
Surgical suture (4.0 silk) with attached needle (1/2 × 17 mm)
Small animal stereotaxic frame with mouse adaptor (KOPF Instruments)
Microprocessor-controlled pump (World Precision Instruments UltraMicroPump) mounted onto the stereotaxic frame
Microprocessor-based controller (World Precision Instruments Micro 1 model)
Small box (we use tip box) taped to the base of the stereotaxic frame, to lay the mouse on
10 μl glass Hamilton syringe with a removable stainless steel blunt-ended 33-gauge needle (Hamilton) (for striatal injection)
5 μl glass Hamilton syringe with a pulled glass microcapillary tube attached (for cerebellar injection): the microcapillary tubes are pulled out on microcapillary needle puller, and cemented to the syringe with Superglue
Drill (Dremel Moto-Tool Model 395 Type 5, or equivalent) with 003 bit
Dissecting microscope (optional)
Lactated Ringer's
3 ml syringe with 25-gauge needle
Recovery mouse cage with clean towel bedding
Lamp with 75 watt bulb, suspended 2.5 feet above the recovery cage
Mouse brain atlas (*The Mouse Brain in Stereotaxic Coordinates,* K. B. I. Franklin and G. Paxinos, Academic Press, 1997)
FIVβgal: concentrated recombinant FIV particles encoding the β-galactosidase transgene, kept on ice

Animal Perfusion/Fixation

Ketamine/xylazine mix (see recipe above)
PBS
2% paraformaldehyde in PBS: in a fume hood, add 2 g paraformaldehyde (powder grade) to near 100 ml of PBS. Cover and heat to 50–60° with stirring. Do not boil. Add a few drops of concentrated NaOH to help dissolution, and bring pH back to 7.4 with concentrated HCl. Bring final volume to 100 ml with PBS. Filter through a 0.45 μm bottle top filter and cool on ice. Store at 4°. Use within 1 week of preparation.

Peristaltic perfusion pump
Flexible rubber hosing 2–3 mm in diameter
Butterfly IV catheter, 23 or 25 gauge
Instruments: scissors, forceps
Styrofoam board
Spray bottle with 70% ethanol

Dissecting Out the Brain

Razor blade or scalpel
Ronguers (Roboz Surgical Instruments)
Curette (spoonlike instrument)
30% Sucrose in PBS
Plastic molds (Peel-a-ways from VWR Scientific Products)
OCT (Tissue-Tek)
Dry ice/95% ethanol bath

Tissue Sectioning

Cryostat
Glass slides (Fisher Superfrost glass plus microscope slides)
Slide boxes
For thick, free-floating sections:
  Forceps
  24-well tissue culture dishes
  PBS
  PBS/azide: PBS with 0.02% sodium azide

Dual Immunofluorescent Staining

Staining of Cryosections on Glass Slides

Humidity chamber (wet paper towels in closed shallow container)
PAP pen (Electron Microscopy Sciences)
PBS
BSA: bovine serum albumin (Sigma, ELISA grade)
Block: PBS with 10% normal (goat) serum (from same species as the secondary antibody), 0.1% Triton X-100, and 0.02% sodium azide (can use 3% BSA in place of or in addition to the serum)
Primary antibody diluent: 3% BSA in PBS with 0.1% Triton X-100 and 0.02% azide
Wash buffer: PBS containing 1% normal (goat) serum, 0.1% Triton X-100, and 0.02% azide
Secondary antibody diluent: PBS containing 1% normal (goat) serum, 0.1% Triton X-100, and 0.02% azide

Primary antibodies:
Polyclonal rabbit anti-β-galactosidase (BioDesign B59136R, 10 mg/ml). Dilute 1/1500.
Mouse mAb to NeuN (Chemicon MAB377, 1 mg/ml). Dilute 1/200.
Mouse mAb to GFAP (Sigma C9205, 1 mg/ml, Cy3 conjugate). Dilute 1/2000.
We purchase this antibody directly conjugated to Cy-3; it works well and eliminates the need for a secondary antibody.
Mouse monoclonal antibody to calbinbin-D-28K (Sigma, ascites). Dilute 1/3000.
Secondary antibodies:
Goat anti-rabbit Alexa 488 (Molecular Probes). Dilute 1/200.
Goat anti-mouse IgG lissamine-rhodamine (Jackson ImmunoResearch). Dilute 1/200.
Glass coverslips
Mounting media: gelmount, or "Vectashield" (from Vector Laboratories, Inc.)
Confocal microscope and associated software

Staining of Free-Floating Thick Sections. The materials are the same as for staining of sections on glass slides except:

The humidity chamber is not needed.
Reagents containing Triton X-100 are prepared with 0.3% Triton X-100 instead of 0.1%.
24-well tissue culture dishes are needed.
A small paint brush is needed.
Glass slides are needed to put sections onto after staining.

Methods

Recombinant FIV Particle Production

We routinely produce recombinant FIV particles utilizing the triple plasmid system and constructs described by Johnston *et al.*[19] (Fig. 1). This system of particle production involves concurrent transfection of TSA201 cells with three plasmids, followed by harvest of particle-containing culture media, and concentration of particles. Below are the steps for preparing 3 ml of concentrated vector particles from an 18 plate (150 mm diameter) transfection.

1. Seed TSA201 cells into 18 150-mm diameter flat-bottom tissue culture dishes at a density of 10^7 cells per dish.
2. The next day, add 34 ml of HBS to two 50-ml conical tubes. The HBS should be at room temperature.

3. Add 225 μg of the packaging plasmid, 337.5 μg of the vector plasmid, and 112.5 μg of the envelope plasmid to each HBS-containing tube and vortex well.

4. Slowly add 1.7 ml of 2.5 *M* $CaCl_2$ to each tube while slowly vortexing or shaking the HBS-plasmid mixture. $CaCl_2$ should be at room temperature.

5. Let the solution stand for 25 min to allow precipitate formation. The solution should appear slightly translucent or cloudy.

6. Add both tubes of precipitate directly to 200 ml of DMEM. Briefly mix.

7. Aspirate off the medium from the cells (9 plates at a time).

8. Gently pipette the transfection solution onto the cells (15 ml per dish), and return the cells to the incubator.

9. Four to 6 h after transfection aspirate off the medium and provide 15 ml of fresh DMEM-10 per dish.

10. Collect the medium (containing vector particles) at 24, 36, and 72 h, replacing this medium with fresh DMEM-10 at the 24 and 36 h time points. At each collection, filter the medium through a 0.45 μm bottle-top filter, and store short-term at 4°, or long-term in 50 ml aliquots at −80°.

11. Just prior to intended use, concentrate the particles by centrifuging the collected medium at 4° for 16 h at 7400*g* (7000 rpm in the Sorvall centrifuge with the SLA 1500 rotor). Carefully pour off the supernatants, drain well, and resuspend particles in lactose buffer. We typically resuspend the particles produced from an 18-plate transfection into a total 3 ml volume.

Comments on FIV Vector Particle Production

1. We have found that transfections work best with CsCl-purified plasmids.

2. We routinely suspend our concentrated particles in PBS/lactose as this buffer is physiological and acceptable for *in vivo* use, and the lactose has a stabilizing effect. However, other buffers maintaining similar pH and salt concentrations may be suitable alternatives. These include saline, TNE (50 m*M* Tris-HCL, pH 7.8, 130 m*M* NaCl, 1 m*M* EDTA), and culture medium.

3. Lentivirus vector-containing culture media suffers minimal loss in transduction titer when stored at −80°, while centrifuge-concentrated vector loses approximately one log in titer after freezing. Substantial loss of titer of concentrated preparations is also observed within 24 h of storage at 4°. Thus we routinely concentrate the virus immediately prior to use.

Determination of Particle Concentration and Transduction Titers

Standardized methods of determining the concentration of FIV-based lentivirus particles and the concentration of transduction-competent particles within lentiviral preparations have not yet been established. An ELISA assay can be used to

measure FIV p24 nucleocapsid antigen,[19,30] as an indicator of particle concentration. For determination of transduction titers, we transduce HT-1080 cells with serially diluted particles, followed by quantification of transduced cells either by staining and counting the transgene-expressing cells, or by quantitative PCR detection of pro-vector DNA sequences.

Determination of Transduction Titer by X-Gal Staining

1. One day prior to transduction, seed a 6-well flat-bottom plate with 2 million HT-1080 cells per well in DMEM-10.
2. For transduction, make a 10-fold dilution series of concentrated FIV as follows. Place 1.485 ml of DMEM-2/polybrene in first tube and 1.35 ml in tubes 2 through 6. Add 15 μl of virus to the first tube and vortex. Transfer 150 μl from the first to the second tube and vortex, and so on for the remaining tubes.
3. Remove medium from wells. Add 1 ml of each dilution to separate wells. For wells #1 through 6, the dilution factors will thus be 10^2, 10^3, 10^4, 10^5, 10^6, and 10^7. Return the cells to the incubator.
4. Incubate the HT-1080 cells for 72 h, then feed with 1 ml of DMEM-10.
5. Incubate a further 24 h. Rinse monolayers with PBS, and then fix with 1% glutaraldehyde for 5 min at room temperature.
6. Wash once with PBS and add enough X-Gal solution to cover the cells.
7. Incubate 6 h in the dark at 37° without CO_2.
8. Rinse the wells 2× with PBS, and add PBS to cover the cells.
9. Using an inverted microscope, count the number of β-galactosidase-expressing (blue) cells in each well. The first two or three wells will often have too many positive cells to count. Doublets or small clusters of cells are counted as one, as they likely originated by division of a single transduced cell.
10. For each well, multiply the total blue cell count by the dilution volume (1 ml) and by the dilution factor. Determine the mean of all the wells. This number represents the transducing units per ml (TU/ml) of concentrated virus. Using this method, our concentrated FIVβgal preparations typically contain 5×10^7 to 10^9 TU/ml.

Determination of Transduction Titer by Quantitative PCR. A PCR-based assay system for titering the FIV vector is described elsewhere.[21] Briefly, HT-1080 target cells are transduced with serial dilutions of FIV vector preparations. The transduced cells are collected 48 h posttransfection, and genomic DNA is extracted according to standard techniques. Total genomic DNA is quantified by staining with Hoechst dye H33258 and comparison with calf thymus DNA standards, using the CytoFluor II fluorometer (PerSeptive Biosystems, Framingham, MA). Quantitative PCR is performed on 100 ng of each DNA sample, employing a PE ABI

[30] G. K. Tilton, T. P. O'Connor, Jr., C. L. Seymour, K. L. Lawrence, N. D. Cohen, P. R. Anderson, and Q. J. Tonelli, *J. Clin. Microbiol.* **28**, 898 (1990).

Prism 7700 system (Perkin-Elmer Corp., Norwalk, CT) and a synthetic oligonucleotide primer set directed against FIV packaging signal sequences yielding an 80-bp product. The resulting fluorescence is used to determine the provector copy number for each HT-1080 DNA sample, and from this the transducing units per ml (TU/ml) of the original concentrated virus is then calculated. Based on the quantitative PCR method, our concentrated FIV preparations typically contain 10^8 to 5×10^9 TU/ml.

Comments on Titering. Titering of transduction-competent particles by staining and counting of transgene-expressing cells can be applied only when a suitable staining method is available. X-Gal staining as described above is a simple and reliable method for detecting β-galactosidase-expressing cells. For other transgene products, immunostaining methods can be applied, assuming there is a suitable antibody available and the HT-1080 cells have low to no endogenous expression of the antigen. X-Gal staining or immunohistochemistry is useful for titer comparison between preparations of the same FIV vector. However, it is not recommended for comparisons between vector preparations carrying different transgenes, as the sensitivities of staining procedures for different transgene products may vary. Titering by PCR requires access to a quantitative PCR system, and effort to optimize the procedure, but once this system is established it can be applied to FIV vectors encoding any transgene. Both titering methods are based on transduction of HT-1080 cells. HT-1080 cell transduction readily occurs with VSV-G-pseudotyped FIV. However, HT-1080 cell transduction may be less efficient if the FIV vector is pseudotyped with a different envelope. Many envelope proteins exhibit restricted cellular tropism, and it might be necessary to identify more suitable cell lines for determining transduction titers of alternate pseudotypes.

Pseudotyping with Alternative Envelopes

We have described here the production of a lentivirus vector pseudotyped with the VSV-G envelope protein. VSV-G lends enhanced structural stability to vector particles, allowing for concentration by ultracentrifugation with minimal loss of infectivity.[27] In addition, VSV-G reportedly mediates viral entry via interaction with a membrane phospholipid component,[31] rather than with a specific cell surface receptor protein, and this imparts VSV-G-pseudotyped vectors with an extremely broad host-cell range, including cells of nonmammalian species.[27] These features have resulted in the common use of VSV-G for pseudotyping MLV and lentiviral gene transfer vectors.

However, there can be disadvantages to using the VSV-G envelope. Despite the wide tropism, VSV-G pseudotyped vectors do not always mediate efficient transduction. For example, VSV-G pseudotyped FIV was unable to transduce polarized airway epithelial cells when applied to the apical surface.[21] Furthermore,

[31] P. Mastromarino, C. Conti, P. Goldoni, B. Hauttecoeur, and N. Orsi, *J. Gen. Virol.* **68**, 2359 (1987).

the observations that VSV-G can be toxic to cells,[27] and that VSV-G pseudotyped vectors are inactivated upon exposure to human serum,[32] may limit the clinical application of VSV-G-pseudotyped vectors. Lastly, particularly for direct *in vivo* applications, widespread tropism can be a drawback when it is desirable to restrict transduction to specific cell types or tissues.

Several reports describe successful pseudotyping of HIV-based lentiviral vectors with alternative envelope proteins. Early HIV-1-vectors were pseudotyped with the MLV amphotropic envelope,[33,34] and the human T-cell leukemia virus envelope,[35] as well as the VSV-G envelope glycoprotein.[34] HIV vectors incorporating envelope glycoproteins from Marburg or Ebola viruses have been produced and show a wide range of infectivity.[36]

Attempts at pseudotyping can also meet with failure. Efficient incorporation of envelope proteins into particles depends on appropriate interaction of cytoplasmic envelope sequences with encapsidated genomes. Maedi-visna virus envelope constructs were unable to pseudotype MLV- or HIV-derived vector particles.[37] Pseudotyping of an HIV vector with the gibbon ape leukemia virus (GaLV) envelope glycoprotein was similarly unsuccessful.[38] However, use of a chimeric construct substituting the cytoplasmic tail of the GaLV envelope with that of the MLV amphotropic envelope protein resulted in the formation of infective GaLV-pseudotyped HIV vectors.[38]

Since FIV and HIV are related lentiviruses, successful pseudotyping of HIV with the aforementioned envelope proteins may predict similar results with FIV vectors. Preliminary studies in our laboratory indicate that FIV vectors can be pseudotyped with unmodified envelope proteins from amphotropic MLV, Marburg virus, and Ross river virus (unpublished observations), and we are currently testing these FIV pseudotypes for cell tropisms in the CNS. Also worthy of mention are a few alternative envelopes described in the literature that, although not reported in combination with lentivirus vectors, have successfully been used to pseudotype MLV vectors. Lymphocytic choriomeningitis virus envelope-pseudotyped MLV particles were structurally stable, withstanding concentration by ultracentrifugation, and exhibited cross-species tropism.[39] Pseudotyping of MLV with the Sendai

[32] N. J. DePolo, J. D. Reed, P. L. Sheridan, K. Townsend, S. L. Sauter, and D. J. Jolly, *Mol. Ther.* **2,** 218 (2000).

[33] K. A. Page, N. R. Landau, and D. R. Littman, *J. Virol.* **64,** 5270 (1990).

[34] J. Reiser, G. Harmison, S. Kluepfel-Stahl, R. O. Brady, S. Karlsson, and M. Schubert, *Proc. Natl. Acad. Sci. U.S.A.* **93,** 15266 (1996).

[35] N. R. Landau, K. A. Page, and D. R. Littman, *J. Virol.* **65,** 162 (1991).

[36] S. Y. Chan, R. F. Speck, and M. C. Ma, *J. Virol.* **74,** 49233 (2000).

[37] U. Zeilfelder and V. Bosch, *J. Virol.* **75,** 548 (2001).

[38] J. Stitz, C. J. Buchholz, M. Engelstadter, W. Uckeret, U. Bloemer, I. Schmitt, and K. Cichutek, *Virology* **273,** 16 (2000).

[39] H. Miletic, M. Bruns, K. Tsiakas, B. Vogt, R. Rezai, C. Baum, K. Kuhlke, F. L. Cosset, W. Ostertag, H. Lother, and D. van Laer, *J. Virol.* **73,** 6114 (1999).

virus fusion protein imparted a restricted tropism for asialoglycoprotein receptor-bearing cells, indicating promise for hepatocyte-directed gene delivery.[40]

The successful production of FIV-based vectors pseudotyped with an alternative envelope may simply involve following the steps outlined above, with a plasmid encoding high-level expression of the alternative envelope protein used in place of the VSV-G envelope plasmid. High-titer production of particles that display appropriate cell tropism would suggest successful pseudotyping. Low titers may indicate poor incorporation of envelope proteins into the particles, or poor receptor expression on the TSA201 or HT-1080 cells. The former problem of incompatibility may be overcome with selective mutations in the envelope protein or construction of chimeric envelopes, whereas the latter problem would necessitate usage of more appropriate cells lines in place of TSA201 and/or HT-1080 cells.

Vector Injection into Adult Mouse Striatum

We have studied the potential of gene transfer to the CNS for treatment of the neurological aspects of lysosomal storage diseases using the MPS VII mouse model. MPS VII is caused by a deficiency of β-glucuronidase, a soluble lysosomal enzyme involved in the degradation of glycosaminoglycans.[4] Like other lysosomal proteins, β-glucuronidase can be secreted and taken up by neighboring cells.[41,42] In the MPS VII (β-glucuronidase-deficient) mouse a single intra-striatal injection of most vectors encoding β-glucuronidase results in local transduction, yet the enzyme penetrates much of the injected hemisphere to provide widespread correction of pathology in both glia and neurons.[43] Vectors encoding the reporter protein bacterial β-galactosidase (a nonsecreted protein) are useful for discerning the vector transduction volume and cell types transduced (see "dual immunofluorescent staining").

Here we describe the steps involved in intrastriatal injection of FIVβgal. Sterile techniques are adhered to for brain injections. The bench space is covered with clean underpads (blue chucks), the surgical instruments are autoclaved, the mouse is prepped with iodine, and the syringe/needle is flushed and incubated with 70% ethanol and rinsed with sterile PBS prior to use. The instruments are dry-sterilized between animals.

1. Preprogram the pump for the appropriate delivery volume and rate.

[40] M. Spiegel, M. Bitzer, A. Schenk, H. Rossmann, W. J. Neubert, U. Seidler, M. Gregor, and U. Lauer, *J. Virol.* **72**, 5296 (1998).

[41] R. M. Taylor and J. H. Wolfe, *Exp. Cell Res.* **214**, 606 (1994).

[42] P. Moullier, V. Marechal, O. Danos, and J. M. Heard, *Transplantation* **56**, 427 (1993).

[43] A. Ghodsi, C. Stein, T. Derksen, G. Yang, R. D. Anderson, and B. L. Davidson, *Hum. Gene Ther.* **9**, 2331 (1998).

2. Anesthetize mice with ketamine/xylazine mix (0.1 ml per 10 g body weight), injected ip. Full anesthesia is achieved in approximately 10 to 15 min. Anesthesia is assessed by firmly pinching a toe; if the mouse exhibits a pedal reflex, anesthesia is not adequate and a second (1/3) dose of ketamine/xylazine is given.

3. Apply eye ointment to eyes. This helps prevent drying, as mice do not blink while under anesthesia.

4. Shave the dorsal aspect of the head and wipe with iodine tincture (be very careful to avoid eyes).

5. Using a scalpel, make a midline sagittal incision through the scalp over the skull to reveal the coronal, sagittal, and lambdoid sutures.

6. Lay the mouse on a small box (or something similar), to bring it up to an appropriate height for the mouse adaptor on the stereotaxic instrument. Firmly secure the head by means of the adaptor palate bar and the nose clamp. Adjust the angle of the palate bar to maintain the skull on a level plane.

7. With the (empty) syringe set into the injector unit, identify bregma as the zero coordinate. For a striatal injection, locate coordinates 0.4 mm rostral and 2.0 mm lateral to bregma, and mark the skull using an ultrafine-tip marker.

8. Remove the syringe, and drill small burr hole through the skull at the mark, being careful to maintain the integrity of the dura.

9. Draw vector into the syringe and set the syringe into the injector unit. Return the syringe to the set coordinates. Prior to lowering the syringe, "fast inject" just until a drop of vector is seen at the needle tip, to ensure proper syringe loading.

10. Lower the syringe through the burr hole until the tip of the needle touches the dura. Slowly insert the needle into the brain parenchyma to a depth of 3.0 mm. Start the microprocessor-controlled pump (preprogrammed to deliver 5 μl at a maximal rate of 500 nl per minute).

11. After vector delivery, leave the needle in place for 5 min, then slowly withdraw (over 5 min).

12. Remove the mouse from the stereotactic apparatus and close the incision with 4.0 silk suture.

13. Inject the mouse with 1 ml of lactated Ringer's subcutaneously to provide hydration during recovery.

14. Place the mouse in a cage with absorbent bedding, warmed by a lamp (75 watt bulb) 2.5 feet above the cage. Drape half the cage with a towel to allow the mouse voluntary escape from the warmth.

15. Monitor the mouse until it is ambulatory, then return it to animal housing.

Comments on Vector Injection into the Striatum. Consultation of a mouse brain atlas is necessary for identification of the skull sutures, bregma, and appropriate injection coordinates. Visualization of bregma may be facilitated by use of a dissecting microscope. Also, use of a dissecting microscope during injection allows visualization of the underlying dura while drilling, reducing the chance of puncture.

Vector Injection into Adult Mouse Cerebellum

The spinocerebellar ataxias (SCA) and other degenerative diseases of the cerebellum are potentially treatable by gene transfer if sufficient numbers of the affected neuronal types can be transduced. Cerebellar Purkinje cells are particularly affected, and as these neurons provide neuronal output for cerebellar control of movement, delivery of a therapeutic gene to these neurons may prevent Purkinje cell dysfunction/death and restore motor function. We have found that one injection of recombinant FIV encoding the reporter β-galactosidase into a cerebellar lobule transduces close to 100% of the Purkinje cells in that lobule.[14,44] Thus an FIV vector encoding a therapeutic molecule has potential clinical value.

For injection of a vector into a cerebellar lobule of an adult mouse, the procedure is essentially as outlined above for "injection into the striatum," with the following modifications. The scalp incision is more posterior with the lambdoid suture centrally revealed. The syringe is cemented with a pulled glass microcapillary tube, rather than a stainless steel needle. This type of needle is very fine, with exterior and interior diameters smaller than those of a 33-gauge stainless steel needle. The cerebellum is organized as a repeated lobular structure. However, the orientation of the lobules may differ between animals. Therefore, rather than using anterior–posterior and lateral coordinates, we choose a lobule in which to inject, then lower the needle into the brain parenchyma at a depth of 1 or 2 mm to dispense the vector (1 to 2 μl) into either the cerebellar cortex or the deep cerebellar nuclei, respectively.

Animal Perfusion/Fixation

The perfusion apparatus should be prepared prior to anesthetizing the first mouse. Set up the pump such that the rubber tubing draws PBS from a container and flushes it out the other end, which is attached to a 23 or 25 gauge butterfly i.v. catheter. Flush the line with PBS to remove all air bubbles from the circuit.

1. Anesthetize the mouse with 0.15 ml of ketamine/xylazine mix per 10 g of body weight, administered i.p. Once deep anesthesia is achieved (see above), place the mouse on its back on a Styrofoam board and tape each paw down.
2. Wet the fur over the abdomen and thorax with 70% ethanol. Using scissors, make a midline cut through the abdominal wall up from the intestinal area to just below the diaphragm, being careful to avoid cutting the underlying viscera. Continue the cut laterally, through the diaphragm (which causes an immediate tension pneumothorax), then up through the ribcage to expose the heart.
3. Using fine scissors, make a small snip in the right atrium.

[44] J. M. Alisky, S. M. Hughes, and S. L. Sauter, *NeuroReport* **11**, back cover (2001).

4. Quickly insert the i.v. catheter into the left ventricle, which can be done easily by poking through the apex of the heart.

5. Turn on the perfusion pump and flush PBS through the mouse, running the blood volume out through the cut right atrium. For a mouse, about 20–30 ml of PBS are sufficient to flush the blood volume out, which is evident by the rapid clearing of the liver from bright red to tan or brown.

6. At this point, turn off the pump and move the hose from the PBS into the paraformaldehyde. It is very important to turn off the pump while changing solutions or air emboli may be introduced that block penetration of the fixative.

7. Restart the pump and run 30–50 ml of paraformaldehyde through the mouse. Adequate fixation is indicated by the occurrence of rapid rigor mortis, due to protein cross-linking. If the mouse is limp, try carefully repositioning the tip of the needle within the left ventricle. Common errors include positioning of the needle bevel in the heart wall or entering the left atrium. Usually repositioning will save the perfusion.

Comments on Animal Perfusion/Fixation. For perfusion/fixation we use a peristaltic pump, which mimics the normal cardiac physiology, to provide thorough permeation of fixative without incurring tissue damage. Syringes or gravity (hanging solutions from the ceiling or from a high shelf) can also be used to deliver the fixative.

Removing the Brain

1. Following perfusion/fixation, decapitate the mouse with a razor blade or scalpel.

2. Use a blade to score the skull anterior to the olfactory bulbs and along the sagittal suture.

3. Using Ronguers, grasp and pull off pieces of skull from around the foramen magnum and surrounding the cerebellum. Continue pulling off pieces of skull until the brain is fully exposed laterally and as far anterior as the olfactory bulbs. Note that this procedure must be done carefully, to avoid damage to the underlying brain. A dissecting microscope may allow better visualization.

4. Use forceps and scalpel to carefully remove remaining dura from the brain surface. Scoop out the brain with a small curette (spoonlike instrument) or similar tool. The adhering olfactory nerves, optic nerves, and cranial nerves should give way with gentle pressure; if not, small scissors can be used.

5. Immerse the brain in paraformaldehyde and postfix overnight at 4°.

6. Transfer into 30% sucrose/PBS. The brain floats initially, but sinks as sucrose diffuses into the tissue. Place at 4° and allow the brain to sink. An intact mouse brain requires approximately 36 h to sink. Permeation of tissue with sucrose serves as a cryoprotectant.

7. Place the brain in a plastic mold. Cover the brain with OCT, and set the mold in a shallow dry ice/95% ethanol bath (do not allow ethanol to mix with the OCT), until the OCT is frozen (whitens upon freezing). Note that sections are cut from the bottom face of the block. Therefore before freezing, the brain can be cut first with a razor blade in the plane desired for sectioning (coronal or sagittal) and the pieces placed with cut sides down in the mold, providing a flat surface for cryosectioning. Alternatively, the whole brain can be immersed in OCT and held with forceps in a desired position until the OCT begins to harden around it.

8. Store the OCT-blocked brain at −80° until it can be cryosectioned.

Tissue Sectioning

1. Peel the plastic mold away from the OCT-blocked brain.

2. Using a cryostat, cut sections (from 8 to 50 μm thick) off the block.

3. If sections are 20 μm or less in thickness, they can be captured directly from the cryostat stage onto glass slides. Two to three sections can be placed on one slide. Slides are kept in the cryostat until the brain has been completely sectioned. The slides are transferred to slide boxes and stored at −20°.

4. For thicker sections (20 to 50 μm), use forceps to grab an edge of the section, and quickly place into a well of a 24-well tissue culture dish with PBS. Store these sections in PBS (short-term) or in PBS/azide (long-term), at 4°.

Dual Immunofluorescent Staining

We routinely use dual immunofluorescent staining and confocal microscopy for examination of transduced cells. Primary antibodies with specificity for neurons or glia can be used along with an antibody specific for the transgene product. We present methods for dual staining of β-galactosidase and NeuN (a marker common to most neuronal types), β-galactosidase and GFAP (a type II astrocyte marker), and β-galactosidase and calbindin (a common marker for cerebellar Purkinje neurons).

The following staining procedure is described for staining of 8 to 20 μm thick cryosections on glass slides. The procedure can be adapted to thicker sections (20 to 50 μm) (see "modifications for staining of free-floating sections").

All incubations are performed in a humidity chamber (which can be as simple as wet paper towels in a closed plastic container), and unless otherwise stated, incubations are at room temperature. Also, to minimize photobleaching of fluorochromes, all incubations subsequent to the addition of fluorochrome-labeled antibodies should be done in the dark.

1. Bring cryosections on glass slides to room temperature, about 10 min. This dries the sections and sticks them firmly to the slides.

or eliminated by titrating down the antibody concentrations and/or modifying the block. When the primary antibody is of the same species as the tissue, the antibody may bind "nonspecifically" to Fc receptor-bearing cells. We have not observed this to be a problem with naive or FIV-injected murine brain, but we have observed high background staining in association with inflammation incurred by other vectors. In this case, it is wise to use mouse-derived primary antibodies directly conjugated to fluorochromes, and to include normal mouse serum in the block.

Analysis of Staining by Fluorescence Microscopy

To determine which cell types are transduced, the stained slides are analyzed first by standard upright fluorescence microscopy to evaluate the quality of the stains, and then by confocal microscopy. With confocal microcopy, fluorescence emission is collected from a subcellular plane (typically 0.3 to 0.5 μm) within a

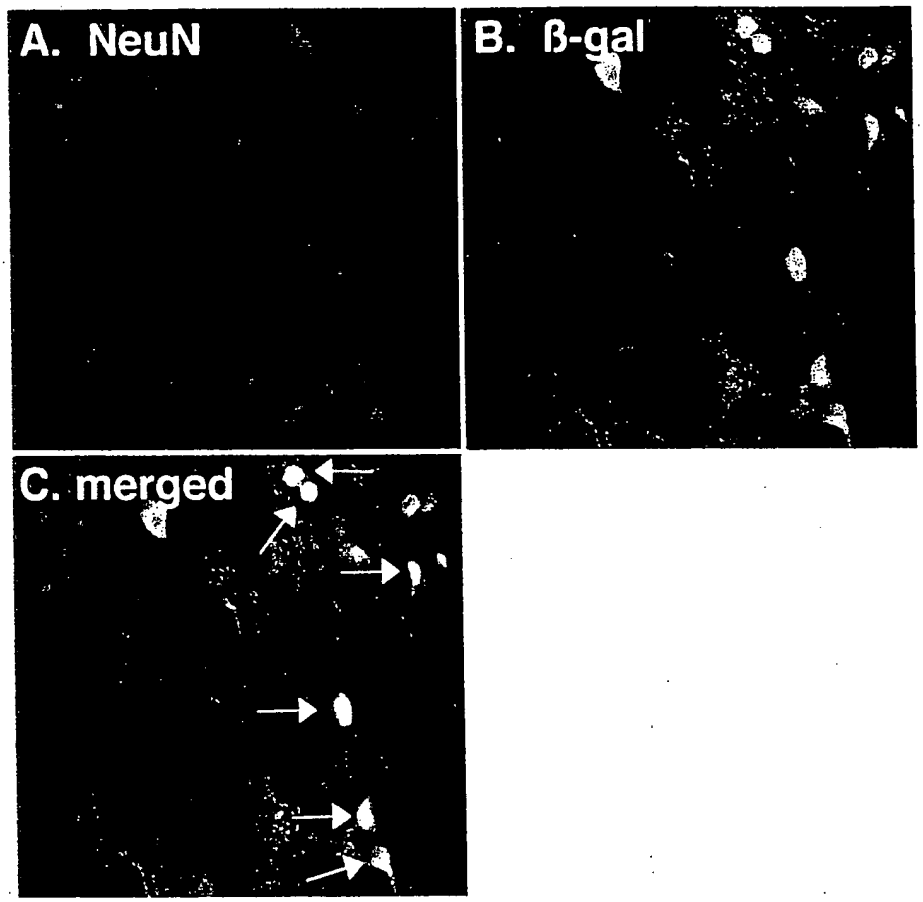

FIG. 2. Dual immunofluorescent staining for β-galactosidase and neurons. FIVβgal was injected into the striatum of a mouse brain. Eight weeks later, 50-μm coronal brain sections were dual stained with a neuronal-specific antibody (A, NeuN, red fluorescence) and a β-galactosidase-specific antibody (B, β-gal, green fluorescence). Overlapping red and green fluorescence appears yellow in the merged images (C) and identifies β-galactosidase-expressing transduced neurons (white arrows).

2. Encircle sections with a PAP pen. Reagents are subsequently applied to slides such that the tissue is completely covered, but the reagent is held within the PAP-defined circle. Usually 100 μl volumes are sufficient to cover one section.

3. Pipette PBS onto slides and incubate for 5 min, to clear the tissue of OCT.

4. Aspirate off the PBS and add Block onto slides. Incubate for 1 h at room temperature.

5. Aspirate off Block and add primary antibodies (diluted in primary diluent). Incubate overnight at 4°.

6. Aspirate off primary antibodies and wash slides 3× with wash buffer, 10 min each.

7. Aspirate off wash and add fluorochrome-labeled secondary antibody(s). Incubate for 1–2 h.

8. Aspirate off secondary antibodies and wash slides 3× with wash buffer, 10 min each.

9. Aspirate off wash buffer and wash 1× with PBS, 10 min.

10. Aspirate off PBS. Add a small volume of mounting medium, and place a glass coverslip over the tissue. Excess mounting medium is removed by inverting the slide onto absorbent paper and applying gentle pressure. Analyze by confocal or standard fluorescence microscopy. Store in dark.

Modifications for Staining of Free-Floating Sections. The following modifications are applied for staining of thick (20 to 50 μm) free-floating sections.

1. Sections are stained (steps 3–9 above) free-floating in wells of a 24-well tissue culture dish. Sections are transferred to fresh wells for each step (use paint brush to transfer).

2. The Triton X-100 in the reagents is increased to 0.3%.

3. The primary antibody incubation time is extended to 48 h.

4. After staining, the sections are placed onto glass slides using a paintbrush. The sections are then coverslipped as described above.

Comments on Immunofluorescent Staining. The above staining procedure was optimized for FIV vector-transduced murine brain. It is important to emphasize that preliminary staining should be performed independently on each antibody to determine optimal concentrations (which can vary from lot to lot or with storage), and that appropriate control stainings be performed to confirm specificity. Negative controls should include concurrent staining of sections with (1) isotype control antibody in place of the antigen-specific primary antibody; and (2) secondary antibody alone (no previous addition of primary antibody). Fluorescence on these sections results from nonspecific binding and indicates that similar nonspecific binding is also occurring on the noncontrol (test) sections, making it difficult to distinguish true antigen-specific staining. Nonspecific binding can be reduced